The Study of Black Hole Properties from Variability of X-ray Emission in Galactic Black Hole X-ray Binaries

Degechisa Abera Regesa

A Thesis Submitted to the Department of Applied Physics

School of Applied Natural Science

Presented in Partial Fulfillment of the Requirement for the Degree of Master's in Applied Physics (Astrophysics)

Office of Graduate Studies

Adama Science and Technology University

October, 2024

Adama, Ethiopia

The Study of Black Hole Properties from Variability of X-ray Emission in Galactic Black Hole X-ray Binaries

Degechisa Abera Regesa

Advisor: Anno Kare (Ph. D)

Co-advisor: Jima Asefa (Ph. D)

A Thesis Submitted to the Department of Applied Physics

School of Applied Natural Science

Presented in Partial Fulfillment of the Requirement for the Degree of Master's in Applied Physics (Astrophysics)

Office of Graduate Studies

Adama Science and Technology University

October, 2024

Adama, Ethiopia

DECLARATION

I declare that this Master thesis entitled "**The Study of Black Hole Properties from Variability of X-ray Emission in Galactic Black Hole X-ray Binaries** " is my own work and has not been submitted to any university for a similar purpose. The references used in this thesis are duly recognized by proper citations.

Degechisa Abera Regesa	____________________	____________________
Name of student	Signature	Date

RECOMMENDATION

We, the advisors of this thesis, hereby certify that we have read the revised version of the thesis entitled "**The Study of Black Hole Properties from Variability of X-ray Emission in Galactic Black Hole X-ray Binaries**" prepared under our guidance by Degechisa Abera Regesa submitted in partial fulfillment of the requirement for the degree of master's of Science in Astrophysics. Therefore , we recommend the submission of the revised version of the thesis to the department following the applicable procedures.

Dr. Anno Kare	______________________	______________________
Advisor	Signature	Date
Dr. Jima Asefa	______________________	______________________
Co-advisor	Signature	Date

APPROVAL PAGE

we, the advisors of the thesis entitled "**The Study of Black Hole Properties from Variability of X-ray Emission in Galactic Black Hole X-ray Binaries**" and developed by Degechisa Abera Regesa, hereby certify that the recommendation and suggestions made by the board of examiners are appropriately incorporated into the final version of the thesis.

Dr. Anno Kare	______________________	______________________
Advisor	Signature	Date
Dr. Jima Asefa	______________________	______________________
Co-advisor	Signature	Date

APPROVAL PAGE

We, the undersigned, members of the Board of Examiners of the final open defense by **Degechisa Abera Regesa** have read and evaluated his thesis entitled *"***The Study of Black Hole Properties from Variability of X-ray Emission in Galactic Black Hole X-ray Binaries***"* and examined the candidate. Therefore, this is to certify that the thesis has been accepted in partial fulfillment of the requirement of the Degree of Master of Science in Applied Physics (Astrophysics).

______________________	______________________	______________________
Chairperson	Signature	Date
Endale Gemechu (PhD)	______________________	December 21, 2024
Internal Examiner	Signature	Date
______________________	______________________	______________________
External Examiner	Signature	Date

Final approval and acceptance of the thesis is contingent upon submission of its final copy to the Office of Postgraduate Studies (OPGS) through the Department Graduate Council (DGC) and School Graduate Committee (SGC).

______________________	______________________	______________________
Department Head	Signature	Date
______________________	______________________	______________________
School Dean	Signature	Date
______________________	______________________	______________________
Office of Postgraduate Studies Dean	Signature	Date

ACKNOWLEDGEMENT

First and foremost, I like offer my sincere and heartfelt gratitude to my GOD for his gift of health and make me be able to do this thesis. I extend my gratitude to my parents and family members, for their continuous guidance, morals, support, encouragement, prayers during my life and advice through my educational achievement at large. Next, my deepest gratitude goes to my major advisor Anno Kare (PhD) and Co-advisor Jima Asefa (PhD) for their strong follow-up that includes instructions, suggestions, and encouragement.

I extend my gratitude to Adama Science and Technology University, School of Applied Natural Science, Department of Applied Physics Program, for providing me with a grant that has financially supported me in carrying out this thesis work. Their support has been invaluable in facilitating the completion of this research. Lastly, I would like to express my deep appreciation to Haramaya University for granting me the opportunity to pursue my studies and enabling me to achieve my academic goals. In conclusion, I am profoundly thankful to all individuals who have played a part, directly or indirectly, in the completion of this thesis.

Contents

List of Tables

List of Figures

LIST ACRONYMS AND ABBREVIATIONS

BHs	Stellar mass black holes
GBHXBs	Galactic Black-hole X-ray binaries
HEASARC	High Energy Astrophysics Science Archive Research Center
HFQPO	High Frequency Quasi-Periodic Oscillation
HMXBs	High mass X-ray Binaries
HS	High state
IS	Intermediate State
ISCO	Innermost stable circular orbit
LMXBs	Low mass X-ray Binaries
LS	Low State
LFQPO	Low Frequency Quasi-Periodic Oscillation
QPO	Quasi-Periodic Oscillation
RXTE	Rossi X-ray Timing Explorer
TOV	Tolman-Oppenheimer-Volkoff
WRLOF	Wind Roche-Lobe Overflow

ABSTRACT

In this study, we investigate the properties of five Galactic Black Hole X-ray Binaries (BHXBs): GRO J1655-40, GX 339-4, XTE J1650-500, XTE J1550-564, and XTE J1118+480, focusing on estimating their black hole masses and spins through X-ray variability analysis. We utilize X-ray light curve data from the All-Sky Monitor (ASM) on the Rossi X-ray Timing Explorer (RXTE), specifically within the 2-10 keV energy range. We identify and characterize Quasi-Periodic Oscillations (QPOs) in the X-ray light curves of these BHXBs and apply theoretical models to estimate black hole masses and spins. For these analyses, we used two primary theoretical models the Resonance model and the Lense-Thirring Precession model. Through fitting these models to the observed QPO frequencies, we derive mass and spin estimates for each BHXB candidate. The results reveal a diverse range of black hole masses, from approximately $5.92 \pm 0.60\, M_{\odot}$ *to* $10.02 \pm 0.12\, M_{\odot}$*. This estimated mass range suggests that these black holes fall within the category of stellar-mass black holes. The GRO J1655-40 and XTE J1118+480 exhibit moderate to low spin values, implying less active accretion processes, while GX 339-4, XTE J1650-500, and XTE J1550-564 show higher spin parameters, indicating a stronger influence of relativistic effects.The consistency of mass estimates derived from both models with each other and with values from prior studies affirms the robustness of the methods used. This study concludes that analyzing X-ray variability, particularly through QPO characterization, provides a powerful tool for investigating the fundamental properties of black holes within BHXB systems.*

Key word: *Black Hole X-ray Binaries, Quasi-periodic Oscillation, mass, Spin*

1

INTRODUCTION

1.1 Background of the study

Black holes are fascinating astronomical objects that have captivated the attention of scientists and researchers for decades. The extreme gravitational field and their mysterious nature make the black holes ideal candidates for studying the fundamental principles of physics and understanding the nature of the universe (Kalamkar et al., 2015). Black holes can be studied when they interact with other stars or other materials. For stellar mass black holes (BHs) the best way to study them is when they reside in binaries and particularly when they accrete material from their companion stars they orbit each other with in black-hole X-ray binaries (Nelemans, 2004). The black hole X-ray binaries (BHXBs) can be used as a source of information about the formation and evolution of black holes as they interact with the environment by emitting the X-rays (Nelemans, 2004). The black hole X-ray Binaries (BHXBs) consist of a black hole and a companion star which they orbit each other in a close binary system (Ingram et al., 2020). The Black hole accretes matter from the companion star and makes an accretion disk, which emits copious amounts of X-ray radiation as the matter spirals towards the event horizon (McClintock and Narayan, 2011). The X-ray emission from black hole X-ray binaries carries crucial information about the black hole, such as the mass of the black hole, angular momentum or spin, and the strength of the magnetic field in the accretion disk (Belloni et al., 2005). The study of these properties of the black hole is vital for advancing our knowledge of black hole formation, growth, and evolution. One of the fundamental properties of a black hole is its mass (Kalamkar et al., 2015). The mass of black hole in BHXBs can be estimated by analyzing the spectral features and applying appropriate models to fit with the X-ray Variability (Qin, 2019). The spin of a black hole is another crucial parameter that influences the behavior of BHXBs (Ingram et al., 2020). The spin affects the structure and dynamics of the accretion disk, which in turn impacts the X-ray spectral and timing properties observed during outbursts (Kalamkar et al., 2015). The spin of a black hole can influence the efficiency of converting accreted matter into energy, which manifests as X-ray emission from the accretion disk. According to (McClintock and Narayan, 2011), the spin parameter can be estimated by analyzing the X-ray emission and applying theoretical models that relate the observed frequencies of Quasi-Periodic Oscillations (QPOs) and the shape of the X-ray spectrum to the black hole's spin. The faster the black hole spins, the closer the material can orbit before crossing the event horizon, affecting the overall energy distribution and luminosity of the system. By studying these X-ray emissions and comparing them with theoretical models like the Lense-Thirring precession or the Resonance model, the spin and mass of the black hole can be estimated. This approach provides critical insights into the relativistic effects near the black hole and helps in characterizing the black hole's fundamental properties.

1.2 Statement of the Problem

Understanding black hole properties, especially mass and spin, is essential for revealing the dynamics and evolution BHXB (Remillard and McClintock, 2006). Given the impossibility of direct observation, scientists study Galactic Black Hole X-ray Binaries (GBHBs), where black holes accrete matter from companion stars, emitting variable X-rays in the process (Esin et al., 1997). This variability includes Quasi-Periodic Oscillations (QPOs), which are linked to the accretion dynamics and provide a window into black hole properties like mass and spin (van der Klis, 1993). However, characterizing black hole properties through QPO analysis presents challenges, such as identifying QPO types amidst noisy data using accurate models to relate QPOs to black hole parameters, ensuring data quality for reliable measurements (Zhang et al., 1994), and understanding the influence of other factors like accretion rates. In this study, we addresses these challenges by identifying and categorizing QPOs across five Galactic BHXB sources using data from the Rossi X-ray Timing Explorer. By applying the Resonance Model and the Lense-Thirring Precession Model to these QPOs, we estimate black hole masses and spins, providing new insights into accretion dynamics across black hole systems.

1.3 Research Objectives

1.3.1 General Objective

The general objective of this thesis is to study Black Hole properties from variability of X-ray emission in Galactic Black Hole X-ray Binaries.

1.3.2 Specific objectives

The specific objectives of this thesis are:

- To identify and characterize QPOs in X-ray light curves in five Galactic BHXBs.
- To estimate the mass of black hole in five Galactic BHXBs.
- To estimate the spin of black hole in five Galactic BHXBs.
- To compare our Black Hole Parameters estimation with previous estimations.

1.4 Significance of the Study

The significance of this study lies in its ability to find way to estimate key parameters such as mass and spin through the analysis of X-ray variability. Using the relationship between Quasi-Periodic Oscillations (QPOs) and the intrinsic properties of black holes, we can gain insights into the dynamics of matter in the extreme gravitational environments surrounding black holes. Additionally, this study contributes to the broader field of high-energy astrophysics by validating theoretical models of QPO generation against observational data. The findings may also have implications for understanding the physics of accretion processes, the behavior of matter in strong gravitational fields, and the fundamental predictions of General Relativity. Ultimately, our study enhances the scientific community's ability to interpret observations of black holes, providing a framework for future investigations into the nature of these enigmatic cosmic objects.

1.5 Scope of the Study

The scope of this research is centered around the analysis of X-ray emissions from stellar mass black holes in BHXBs. The study excludes investigation of supermassive black holes and does not involve analysis of other wavelengths of the electromagnetic spectrum. The primary objectives include analyzing X-ray observables from Galactic BHXBs and estimating key properties of the black holes within them. The research focuses on five well-established Galactic BHXB candidates: GRO J1655-40, GX 339-4, XTE J1650-500, XTE J1118+480, and XTE J1550-564. The analysis of the collected X-ray data employed X-ray timing analysis techniques using the different Python package, enabling the fitting of observed X-ray properties with theoretical models like the Resonance and Precession models. Through this approach, the research estimates crucial physical parameters of the black holes, including their masses and spin.

2

LITERATURE REVIEW

2.1 Formation and types of Black-Hole X-ray Binaries

The formation of a black hole X-ray binary (BHXB) begins with the evolution of a binary star system (Brown and Lee, 2001). Over time, the primary star in this system exhausts its nuclear fuel and undergoes a supernova explosion as seen from figure 2.1. If the remnant's mass exceeds the Tolman-Oppenheimer-Volkoff (TOV) limit, it collapses into a black hole; otherwise, it becomes a neutron star (Nampalliwar and Bambi, 2019). In the case of a black hole, the companion star continues to evolve. As the companion star expands into the red giant phase, it can overflow its Roche lobe, leading to mass transfer from the companion to the black hole (Brown and Lee, 2001). This process, known as Wind Roche-Lobe Overflow (WRLOF), allows material to be transferred to the black hole, forming an accretion disk (Nampalliwar and Bambi, 2019; Levina et al., 2023). The accretion disk consists of gas and dust spiraling inward under the immense gravitational pull of the black hole, emitting high-energy X-rays due to heating and compression. BHXBs are classified into two main types based on the mass of the companion star: Low Mass X-ray Binaries (LMXBs) and High Mass X-ray Binaries (HMXBs).

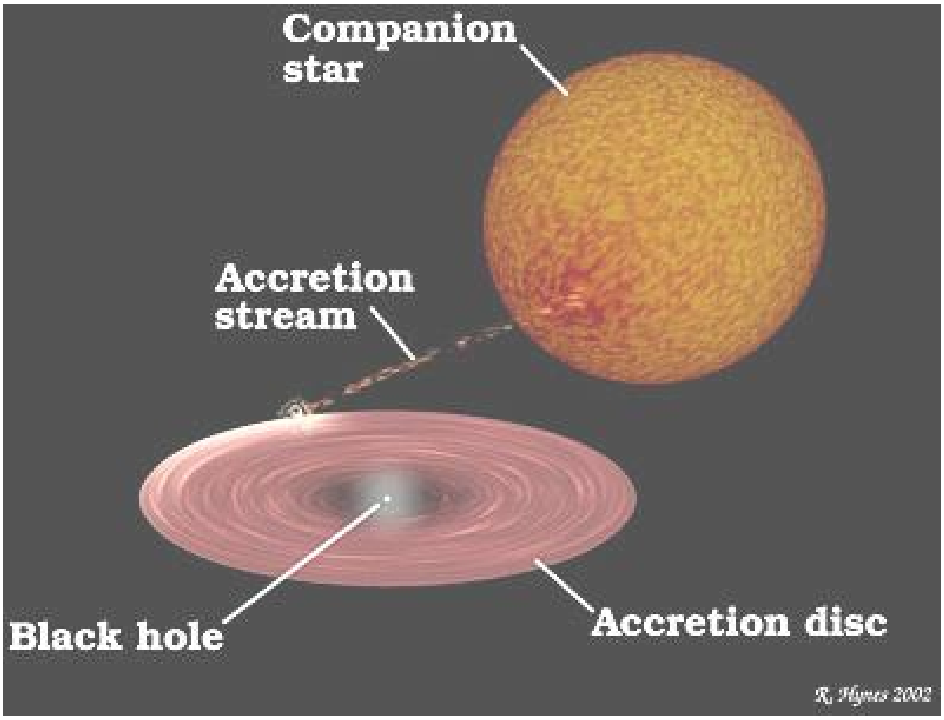

Figure 2.1: Black Hole X-ray Binary form With Companion Star and Accretion Disk. Source: https://universe-review.ca/F08-star17.htm.

2.1.1 Low mass X-ray Binaries(LMXBs)

In LMXBs, the black hole orbits a low-mass companion star, typically a main-sequence star or a white dwarf (Nampalliwar and Bambi, 2019). As these systems evolve, the companion star reaches a point where its outer layers are gravitationally bound to the black hole, spilling matter into the black hole's gravitational field through Roche-lobe overflow (Orosz and Bailyn, 1997). This infalling material forms an accretion disk around the black hole, where viscous processes drive the inward flow of matter, releasing thermal X-ray emission (Wijbrands and van der Klis, 1999). LMXBs exhibit both bursts and continuous X-ray emission, reflecting the dynamic nature of their accretion processes.

2.1.2 High mass X-ray Binaries(HMXBs)

In contrast, HMXBs involve a black hole orbiting a more massive companion star, often an O or B-type star (Nampalliwar and Bambi, 2019). These stars possess strong stellar winds, and the black hole captures material from these winds in a process known as Bondi-Hoyle accretion (McClintock and Remillard, 2009). HMXBs typically have complex and turbulent accretion flows due to interactions with the black hole's magnetic field, resulting in non-thermal X-ray emission (Wijbrands and van der Klis, 1999). Like LMXBs, HMXBs can exhibit diverse behaviors, including both continuous and bursting X-ray emissions.

2.2 The spectral states of Black Hole X-ray binaries

The black-hole binaries can be well described with several distinct X-ray states, some of them being associated with jet launching. A full evolution cycle of the state transition can be observed with convenient timescales like months to years, which was well explained as the evolution of accretion disk. The structure of accretion flows depends primarily on the Eddington ratio. According to (Ajayi et al., 2016) when the Eddington ratio fluctuates, the accretion flow transitions dramatically into different states, each with distinct geometries and spectral characteristics. Both LMXBs and HMXBs can exhibit spectral state transitions, where the X-ray emission characteristics change dramatically. These transitions are associated with changes in the accretion rate and the relative importance of different emission mechanisms (McClintock et al., 2003). Understanding these transitions is crucial for unraveling the complex interplay between the black hole, the accretion disk, and the companion star. BHXB basically classified to three distinct spectral states in order of increasing luminosity, these are the low state, intermediate state and high state (McClintock et al., 2003).

2.2.1 Soft/high state

In stellar-mass black hole with further increase of Eddington ratio, the accretion flow becomes hot and luminous, it emits Soft-X-ray emission with a thermal spectrum (Wang et al., 2012). Soft state has a strong blackbody component and no discernible high-energy cutoff in the spectral tail beyond the blackbody. In soft state the thermal spectrum of the disk is the dominant component in the spectrum and the inner part of the disk temperature is around 1keV. If the luminosity of the source is between upto 5 to upto 30 of its Eddington luminosity, the disk inner edge is at the ISCO and the accretion disk should be well described by the Novikov-Thorne model. In the soft state, we do not observe any kind of jet. However, strong winds and outflows are common (while they are absent in the hard state). The luminosity of the source may somewhat decrease and the hardness may change, while remaining on the left side of the HID (Nampalliwar and Bambi 2019). The detailed form of spectra of weak states remains uncertain, with some observations showing $\Gamma > 2$, like XTE J1118+480. The soft state is often subdivided into the high (HS), very high (VHS) and intermediate (IS) states. The high or ultrasoft, state is thought to consist solely of the blackbody disk component and not include a high-energy tail; however, this characterization is obviously contingent upon the instrument's sensitivity. In actuality, high-energy tails are found in the majority of spectra that are said to represent this condition (Zdziarski and Gierliński, 2004).

2.2.2 Intermediate states

The intermediate state occurs during the hard-soft state transitions, and it is characterized spectrally by the high-energy tail starting close to the peak of the disk blackbody (Zdziarski and Gierliński, 2004). Intermediate state corresponds an unstable accretion flow. In the intermediate state, the accretion will have an extremely high or super-Eddington accretion rate, its accretion disk is described as a slim disk. For this reason, the intermediate state is also called the very high state (Ajayi et al., 2016). The mass accretion rate rises, so the contribution of the thermal component increases. The power-law and the reflection components get weaker, probably because of a variation in the geometry/properties of the corona. As a consequence, the source moves to the left part of the hardness-intensity diagram (HID). For the Intermediate state we have the hard-intermediate state at the beginning and the soft-intermediate state then. During the transition, transient highly relativistic jets are observed (Nampalliwar and Bambi, 2019).

2.2.3 Hard/low state

The hard state, also known as low, or LS, is characterized by a weak soft blackbody component and a high-energy spectral cutoff at > 100 upto 200 keV (Ann A.Esin, Jeffrey E. Mcclintock 1997). A wide range of the Eddington ratio, up to L/LE 0.2 upto 0.3, where LE 1.5 × 1038(M/M0) erg s 1, can lead to the hard state (McClintock and Remillard, 2009). At the beginning of the outburst, the spectrum is hard and the source becomes brighter and brighter because the mass accretion rate increases (L/LEdd starts from 10 upto 3 and can reach values up to 0.7 in some cases). The spectrum is dominated by the power law and reflection components. The thermal component is subdominant, and the temperature of the inner part of the disk may be low (0.1 keV or even lower), but it increases as the luminosity of the source rises. The inner edge of the disk is initially farther away than the ISCO, but it moves to the ISCO as the luminosity increases, and it may reach the ISCO at the end of the hard state.

2.3 X-ray Emission from Black-Hole Binaries

2.3.1 Accretion Disks in Black Hole X-ray Binaries (BHXBs)

Accretion disks are crucial components of black hole X-ray binaries (BHXBs) as they fuel their intense radiation across the electromagnetic spectrum, including X-rays. These swirling disks of gas and dust from around the black hole, continuously replenished with material captured from a companion star. The immense gravitational pull of the black hole draws this material inwards, causing it to heat up due to viscous dissipation (Shakura and Sunyaev, 1973). Several mechanisms contribute to the formation of these accretion disks. Roche lobe overflow is a major process, where the companion star fills its Roche lobe, the region bound to the black hole by gravity (Authors, 2020). As the star evolves and expands, the excess material spills over and is captured by the black hole's immense gravity. In stellar wind capture the black hole captures charged particles expelled from the stellar wind of the companion star. These particles then lose angular momentum and spiral inwards towards the black hole, contributing to the accretion disk's growth. According to (Fabian et al., 1989) star can be ripped apart by the tidal forces of a very close encounter with a black hole in a tidal disruption event. This catastrophic event results in the immediate formation of a massive accretion disk around the black hole, leading to intense X-ray emission. Once captured by the black hole, the material in the accretion disk experiences immense friction as it spirals inwards. This friction heats the disk to millions of degrees, causing it to emit thermal radiation across the electromagnetic spectrum, including X-rays.

2.4 X-ray emission mechanisms

X-ray emitted from accreting black hole binaries in two main components: thermal and non-thermal. Thermal X-ray emission is primarily produced by optically thick accretion flows, where the gravitational energy of matter is converted to photons of X-ray wavelengths. This thermal component is typically observed in the soft X-ray band and is characterized by a thermal spectrum with a characteristic temperature of a few keV. Non-thermal X-ray emission, on the other hand, is expected to arise from particle acceleration in buoyant magnetic loops. This non-thermal component is commonly observed in the spectra of black hole candidates and has a power law-shaped hard X-ray component with a photon index of $\Gamma \approx$ 2-3. The non-thermal component is often observed in the hard X-ray band and is thought to be produced by inverse compton scattering of soft photons by energetic electrons. Additionally, non-thermal processes in optically thin media, such as comptonization on the non-thermal tail of the electron distribution, may also contribute to the X-ray emission from black holes in some spectral states. These processes are thought to be responsible for the hard X-ray tails observed in some black hole candidates, which extend up to energies of several hundred keV.

2.4.1 Bremsstrahlung radiation

Bremsstrahlung, which means "braking radiation" in German, occurs when charged particles are accelerated or decelerated by the electric fields of other particles. The charged particles in the accretion disk surrounding the black hole experience the strong gravitational field of the black hole. As these particles interact with the black hole's gravity, they are accelerated or decelerated, resulting in the emission of electromagnetic radiation. The bremsstrahlung process is particularly significant for X-ray emission because the high energies involved in the interaction of charged particles near a black hole can produce X-ray photons. The emitted X-ray photons arise from the deceleration of charged particles, such as electrons or ions, as they interact with the intense gravitational field of the black hole (Gilfanov, 2009).

2.4.2 Compton scattering

Compton scattering occurs when a high-energy photon interacts with a charged particle, usually an electron, resulting in a change in the photon's energy and direction. High-energy photons originating from the inner regions of the accretion disk or near the black hole itself interact with electrons in the outer regions of the disk. These interactions can occur in the so-called "corona," a hot and tenuous region above or below the accretion disk, where high-energy particles are present. The compton scattering process leads to the upscattering of lower-energy photons to higher energies, shifting them into the X-ray regime. The scattered X-ray photons carry information about the energy distribution and properties of the electrons in the corona.

2.4.3 Magnetic reconnection

Magnetic reconnection is a process that can contribute to the production of X-ray photons. It occurs when twisted or tangled magnetic field lines in the accretion disk undergo a sudden rearrangement, releasing a significant amount of stored magnetic energy. Can occur in regions where the magnetic field lines become highly stressed or twisted. As the magnetic field lines rearrange themselves to achieve a lower energy configuration, the stored magnetic energy is converted into other forms, including the kinetic energy of charged particles (Wijbrands and van der Klis, 1999). During magnetic reconnection, charged particles, such as electrons or ions, can be accelerated to high energies. These accelerated particles emit synchrotron radiation as they spiral along the magnetic field lines, which can extend into the X-ray band. Synchrotron radiation refers to the emission produced when charged particles are accelerated or deflected in strong magnetic fields.

2.4.4 X-ray reflection

X-rays emitted from the inner regions of the disk or near the black hole can interact with the denser regions of the outer disk, resulting in reflection. When X-rays encounter the denser material in the outer regions of the accretion disk, such as gas or dust, they can undergo several interactions, including scattering and absorption. Some of the X-rays are scattered or absorbed, while others are reflected back towards the observer. The process of X-ray reflection can be described by the reflection spectrum, which provides information about the properties of the reflecting material. The reflection spectrum is characterized by several features, including a broad hump known as the compton hump, iron Kα emission lines, and absorption edges.The reflection spectrum can be modeled using physical parameters such as the iron abundance, ionization state, and geometry of the reflecting material. The intensity of the reflected X-rays depends on the incident X-ray flux, the reflection efficiency, and the geometry of the reflecting surface (Fabian et al., 1989)

2.5 Observational Signatures of X-ray Emission from Black-Hole Binaries

2.5.1 Characterization of X-ray Emission from Accreting Black Holes

X-ray emission from accreting black holes is characterized by a power-law spectrum with a spectral index that ranges from about 1.5 to 2.5. This is one of the key features of X-ray emission from black-hole binaries. The power-law component is often attributed to comptonization of soft photons by hot electrons in the accretion flow, although the exact physical mechanism is still a matter of debate. The spectral index of the power-law component can vary depending on the state of the accretion flow, with values ranging from about 1.5 in the soft state to about 2.5 in the hard state (Gilfanov, 2009).

2.5.2 Variability of X-ray Emission from Accreting Black Holes

The X-ray emission from black-hole binaries is known to be variable, and this variability can be characterized by a number of different timescales. This is another key feature of X-ray emission from accreting black holes. The amplitude of flux variations can be as large as 20-30 fractional rms, and the dependence of the variability amplitude on timescale is conventionally characterized by the power density spectrum. The power density spectrum is a square of the Fourier-amplitudes of the time series, re-normalized in order to give the answer in desired units, for example (fractional rms)2/Hz. The energy dependence of the variability can be characterized by the frequency-resolved energy spectrum, which is defined as a set of Fourier-amplitudes computed from light curves in different energy channels. The study of the variability properties of X-ray emission from black-hole binaries is an important tool for understanding the underlying physical processes, as well as for testing theoretical models (Barret et al., 2000). Using the timescale, TB, as a representation of black hole accretion was established with the finding of a correlation between TB and black hole mass MBH was established by Again, it was strengthened as the break timescale is also correlated with spectral states or luminosities of XRBs. TB is a good reflector of black hole masses and accretion states (in terms of bolometric luminosity Tbol) (Ajayi et al., 2016).

2.5.3 Correlations of X-ray Emission with Black-hole X-ray Binary Properties

The X-ray emission from black-hole binaries is correlated with other properties of the black-hole binary, such as the mass of the black hole and the mass transfer rate from the companion star. This is another important feature of X-ray emission from accreting black holes, as discussed by (Town, 2014). The X-ray luminosity of black-hole binaries is known to scale with the mass transfer rate from the companion star, and this relationship is often used to estimate the mass transfer rate from the observed X-ray luminosity. The X-ray luminosity is also known to scale with the mass of the black hole, with more massive black holes producing more luminous X-ray emission. The spectral and timing properties of the X-ray emission are also known to depend on the state of the accretion flow, which is in turn related to the mass transfer rate and other properties of the binary system. The study of the correlations between X-ray emission and other properties of black-hole binaries is an important tool for understanding the underlying physical processes, as well as for testing theoretical models (Tetarenko et al., 2020).

2.6 Cataloging candidates of black holes in X-ray binaries

2.6.1 GRO J1655-40

GRO J1655-40 is a well-studied X-ray binary star system, first discovered by NASA's Compton Gamma Ray Observatory (CGRO) in 1994 (Zhang et al., 1994). This system consists of a black hole and a normal stellar companion. The black hole in GRO J1655-40 source estimated to have a mass 5-7$M_\odot$ by (Orosz and Bailyn, 1997) and 6.30 ± 0.27$\odot$ by (Wang et al., 2012). (Dunn et al., 2010) also estimated the Black Hole in this source as 7.0 ± 0.2$M_\odot$ and its distance as 3.2 ± 0.2 kpc in their study. The companion star in this source is a subgiant with a mass of approximately 2-2.5$M_\odot$ (Beer and Podsiadlowski, 2002). The black hole in GRO J1655-40 accretes matter from its companion star through an accretion disk, which emits X-rays due to the intense gravitational forces heating the in-falling material (Remillard and McClintock, 2006). These X-ray emissions are crucial for studying the physical mechanisms in the accretion disk, including the dynamics of the disk, the behavior of matter under extreme gravitational forces, and the processes of energy dissipation and angular momentum transfer. High-energy observations from this source have revealed complex variability patterns and spectral features that provide insights into the conditions and processes within the accretion disk (Homan et al., 2005). GRO J1655-40 undergoes periodic outbursts, where the X-ray and radio emissions significantly increase. These outbursts are believed to be caused by changes in the accretion rate and instabilities within the accretion disk (Maccarone and Coppi, 2002). (Beer and Podsiadlowski, 2002) studied the distance of GRO J1655-40 as 3.2 kpc and (Hjellming and Rupen, 1995) suggested in their study that the distance of 3.2 kpc from (Beer and Podsiadlowski, 2002) is more accurate. Numerous studies have focused on this system to understand black hole physics and accretion processes dynamics (Remillard and McClintock, 2006).

2.6.2 GX 339-4

The Galactic X-ray binary GX 339-4 is an extensively studied low-mass X-ray binary (LMXB) system that was first discovered in 1972 by the MIT OSO-7 satellite (Markert et al., 1973). The system consists of a stellar-mass black hole and a low-mass companion star. In their study (Heida et al., 2017) estimated the mass of black hole in GX 339-4 system as 5.8-6.5 $M_\odot$ and (Wang et al., 2012) as 5.8 ± 0.5$M_\odot$. (Dunn et al., 2010) also estimated the Black Hole mass in this source as 5.8 ± 0.5$M_\odot$ which is complementary to what (Wang et al., 2012) estimated. The companion star in the source believed to be a low-mass main-sequence star with a mass less than 1$M_\odot$. GX 339-4 is located at a distance of approximately 8.0 ± 4.0 kiloparsecs (kpc) from Earth according to studies from (Dunn et al., 2010). The system is known for its complex variability and exhibits several different states, including quiescent, low/hard, intermediate, and high/soft states (Belloni et al., 2005). These states are characterized by different levels of X-ray emissions, which are indicative of changes in the accretion rate and the structure of the accretion disk around the black hole. The X-ray emission from GX 339-4 often shows variability on timescales ranging from milliseconds to months, which is used to investigate the dynamics of the inner accretion disk, including the processes of energy dissipation, angular momentum transport, and the effects of strong gravitational fields (Homan et al., 2005). Periodic outbursts are a significant feature of GX 339-4. Over 43 years, GX 339-4 has undergone 20 outbursts, during which the entire array of spectral accretion states has been observed (Belloni et al., 2005). These outbursts, during which the system's X-ray luminosity can increase by several orders of magnitude, are thought to be caused by instabilities in the accretion disk leading to a rapid increase in the mass accretion rate (Tetarenko et al., 2016). GX 339-4 is one of the few black hole binaries that have been observed to undergo state transitions multiple times (Fender et al., 2004).

2.6.3 XTE J1650-500

Galactic Black Hole X-ray Binary XTE J1650-500 is a low-mass X-ray binary (LMXB) system that was first discovered by the Rossi X-ray Timing Explorer (RXTE) in 2001 (Remillard et al., 2002). The system consists of a black hole and a low-mass companion star. The black hole in XTE J1650-500 has a mass of around 6 ± 3 $M_\odot$ as it estimated by (Dunn et al., 2010) in their study. The system is located at a distance of approximately 2.6 kiloparsecs (kpc) from Earth (Homan et al., 2006). This relatively close distance allows for detailed observational studies providing critical insights into the behavior of black hole binaries. XTE J1650-500 is known for its significant variability and exhibits several different states, including quiescent, low/hard, intermediate, and high/soft states (Homan et al., 2003).

These states are characterized by different levels of X-ray emissions, which are indicative of changes in the accretion rate and the structure of the accretion disk around the black hole. The X-ray emission from XTE J1650-500 is critical for studying the physical mechanisms within the accretion disk. The emission often shows variability on timescales ranging from milliseconds to months, which is used to investigate the dynamics of the inner accretion disk (Homan et al., 2003). These observations have revealed complex variability patterns and spectral features that provide insights into the conditions and processes within the accretion disk (Miller et al., 2002). Periodic outbursts are a significant feature of XTE J1650-500. These outbursts, during which the system's X-ray luminosity can increase by several orders of magnitude, are thought to be caused by instabilities in the accretion disk leading to a rapid increase in the mass accretion rate (Cui et al., 2002).

2.6.4 XTE J1550-564

XTE J1550-564 is a Galactic Black Hole Binary, first detected by the RXTE All-Sky Monitor (ASM) (Rodriguez et al., 2002). The system's rapid X-ray variability, hard spectrum, and lack of X-ray bursts or pulsations initially indicated it as a black hole candidate (BHC) XTE J1550-564 has experienced five major outbursts in 1998/1999, 2000, 2001, 2001/2002 and in 2003 according to (Tetarenko et al., 2016). The initial two outbursts displayed a typical pattern characteristic of black hole state transitions. The subsequent three outbursts were less luminous and remained in the hard state (Belloni et al., 2002; Sturner and Shrader, 2005). (Orosz et al., 2004) presented a refined dynamical model, including parameters such as the orbital period (P_{orb}), mass function ($f(M)$), mass ratio (q), and inclination (i). Their analysis, based on photometric and spectroscopic data over seven years, identified the inclination angle range as 57.7° < i < 77.1°. However, they noted the potential unreliability of these measurements due to non-simultaneous light fraction determinations. Utilizing the data and methodologies with an isotropic distribution over the inclination range (Dunn et al., 2010) estimated the black hole mass in XTE J1550-564 as 10.6 ± 1.0 M$\odot$ and its distance from Earth as approximately 5.3 kiloparsecs (kpc). In their study (Wang et al., 2012) estimated the mass of Black Hole in this source as 9.7 - 11.6M$\odot$ and its distance as 5.6 kpc.

2.6.5 XTE J1118+480

Galactic Black Hole X-ray Binary XTE J1118+480 is low-mass X-ray binary (LMXB) system that was first discovered in 2000 by the Rossi X-ray Timing Explorer (RXTE/ASM) (Remillard et al., 2000). The system consists of a stellar-mass black hole and a low-mass companion star. Dynamical measurements established a large mass function ($>$6 M$\odot$) confirmed a BH primary in this system (Wagner et al., 2001). In their study (Khargharia et al., 2013) also estimated the black hole mass in XTE J1118+480 source as approximately 6-7.5M$\odot$(Khargharia et al., 2013) and 6.8 ± 0.4M$\odot$Dunn et al., 2010. XTE J1118+480 is located at a distance of about 1.72 kiloparsecs (kpc) from Earth (Gelino et al., 2006). The system is known for its significant variability and exhibits several different states, including quiescent, low/hard, intermediate, and high/soft states (McClintock et al., 2003). XTE J1118+480 has been extensively observed in the X-ray regime, providing valuable information about the physical mechanisms within the accretion disk. The X-ray emission from XTE J1118+480 often shows variability on timescales ranging from milliseconds to months, which is used to investigate the dynamics of the inner accretion disk (Wagner et al., 2001). XTE J1118+480 exhibits periodic outbursts, during which the system's X-ray luminosity increases by several orders of magnitude (Hynes et al., 2000). These outbursts are caused by instabilities in the accretion disk leading to a rapid increase in the mass accretion rate (Zurita et al., 2002).

3

METHODOLOGY

3.1 Sample Selection and Data Source

3.1.1 Criteria of Source Selection and Selected Sources

We selected a sample of five Galactic Black Hole X-ray Binaries (BHXBs) from the ASM/RXTE satellite data. This selection was guided by studies including (Wang et al., 2012, Dunn et al., 2010, Remillard and McClintock, 2006), as well as the latest Low-Mass (Liu et al., 2001) and High-Mass X-ray Binary Catalogs (Liu et al., 2007). Our primary criteria included strong, consistent X-ray emissions and confirmed evidence of black holes, based on dynamical mass measurements or optical counterpart studies. To ensure reliable timing analysis and robust black hole parameter estimation, we prioritized sources with high-quality light-curve data from the ASM/RXTE archive. These data featured a high signal-to-noise ratio (SNR), which allowed for the precise detection of X-ray variability. The selected BHXBs also had to exhibit different X-ray states (low/hard, high/soft, and intermediate), providing comprehensive insight into the physical processes occurring around the black hole. In order to enable consistent and comprehensible analysis, we additionally took into account elements such as low contamination from adjacent X-ray sources and well-established historical behavior. In order to accurately represent the emission parameters of the sources, they also have to be detectable and well-observed within the ASM/RXTE energy range (2-10 keV). The following five BHXBs were selected for our investigation based on these criteria: GRO J1655-40, GX 339-4, XTE J1650-500, XTE J1550-564, and XTE J1118+480 (Remillard and McClintock, 2006). This method made sure the sources chosen satisfied all requirements for deriving significant information on the characteristics of black holes.

3.1.2 All Sky Monitor on The Rossi X-ray Timing Explorer (RXTE)

The Rossi X-ray Timing Explorer (RXTE), launched on December 30, 1995, was a mission focused on studying high-energy X-rays emitted by objects like black holes, neutron stars, and other extreme environments in the universe. RXTE's mission spanned over 16 years, until January 1, 2012, and its data continue to provide valuable insights into the dynamics of Black Hole X-ray Binaries (BHXBs) (American and Society, 2000).

Figure 3.1: NASA's RXTE satellite with ASM, PCA, and HEXTE instruments. Source: NASA (1996).

As it is seen from figure 3.1 RXTE utilized several instruments, including the All-Sky Monitor (ASM), which played a crucial role in our study. The ASM continuously scanned the sky, covering approximately 80% every 90 minutes, with a spatial resolution of 3' x 15' (Vrtilek, 2004). Its three Scanning Shadow Cameras (SSCs) allowed for the detection and monitoring of X-ray sources across the entire sky, producing valuable X-ray light curve data for hundreds of celestial objects, including BHXBs (Levine et al., 1996). We used X-ray light curve data of Five Galactic BHXBs from the ASM which covers during the entire operation of the RXTE satellite from 1996 to 2012. This data was provided in ASCII format by MIT's ASM

X-ray Light Curves database, and it offers detailed information on the variability of X-ray emissions in these systems. The ASM's high duty cycle and wide sky coverage allowed for multiple daily observations of these sources, ensuring a robust dataset for our analysis. This extensive data allowed us to track the X-ray activity of the BHXBs over the entire operational period of RXTE, enabling us to investigate the long-term variability and behavior of the black holes within the 2-10 keV energy range.

3.2 Materials/Software Used

To analyze the ASM/RXTE data for the selected Black Hole X-ray Binaries (BHXBs), we employed a suite of Python packages and libraries. These tools facilitated data processing, visualization, and model fitting. We utilized `Astropy-v5.3.4` for managing our data and performing time and coordinate transformations necessary for processing the X-ray light curves obtained from the ASM/RXTE archive. `NumPy` (Harris et al., 2020) and `SciPy` (Virtanen et al., 2020) were used for numerical operations and scientific calculations. `NumPy` facilitated efficient array manipulations and mathematical functions required for data handling, while `SciPy` supported optimization tasks, particularly in fitting theoretical models to observed Quasi-Periodic Oscillation (QPO) frequencies, aiding in the estimation of black hole Parameters. For visual representation of our data and analysis results, we used `Matplotlib` (Hunter, 2007). This library enabled us to plot X-ray light curve's Power Density Spectra (PDS), Lorentzian fits, and the resulting black hole parameter estimations. Effective visualization was crucial for illustrating the alignment between observed data and theoretical models. `Pandas` (McKinney, 2010) was utilized for data preprocessing tasks, including filtering and sorting the X-ray light curves to exclude irrelevant radiation and ensuring that our datasets were clean and suitable for subsequent analysis. Advanced model fitting was conducted using the `lmfit` package (Newville, 2014). This tool allowed us to fit Lorentzian models to the PDS, extract accurate QPO parameters. Through minimizing the differences between observed and theoretical frequencies, `SciPy` ensured precise estimation of black hole parameters. The integration of these software tools was orchestrated to create a seamless workflow. The combination of these Python packages and libraries was essential in achieving our research objectives, enabling robust analysis of X-ray emissions from BHXBs and accurate estimation of black hole properties.

3.3 Preprocessing of X-ray Light Curve Data

To analyze the X-ray light curve data of Galactic Black Hole X-ray Binary (BHXB) candidates retrieved from the ASM/RXTE satellite database, we first performed background subtraction by subtracting the provided background counts from the intensity for each row of each source. Next, we applied a series of filtering steps as outlined by (Corcoran, 2004). Using the `Pandas` library in Python, we effectively manipulated and filtered the data to ensure its quality and reliability for further analysis. The specific filtering criteria applied to the X-ray light curve data were as follows: Data points were considered only if the number of sources in the field of view was less than 16, helping to minimize confusion and contamination from other X-ray sources, ensuring that the X-ray light curve primarily reflects the behavior of the targeted BHXB candidates. We selected only data points with an exposure time greater than 30 seconds, as longer exposure times enhance the signal-to-noise ratio, leading to more reliable measurements of the source's X-ray flux. The data were filtered to include only those points where the long-axis angle, θ, was between -41.5 degrees and 46 degrees. This range ensures that the instrument's pointing is within optimal limits, reducing the likelihood of systematic errors. Lastly, data points with a short-axis angle, ϕ, between -5 degrees and 5 degrees were retained, ensuring that the source is well-centered in the field of view, enhancing the accuracy of the measurements. Using the `Pandas` library, we implemented the above filtering criteria to process the raw data. The filtered data using these steps are summarized in Table 3.1, which illustrates the reduction in data points for each Galactic BHXB source after applying the quality filters. The resulting preprocessed light

Table 3.1: Number of Data Points for Each BHXB Source Before and After Filtering

Source	Data Points (Before)	Data Points (After)
GRO J1655-40	8,704	6,441
GX 339-4	2,480	2,295
XTE J1650-500	14,642	13,543
XTE J1550-564	4,662	3,197
XTE J1118+480	41,698	32,366

curve dataset ensures that our subsequent analyses, including Power Density Spectrum (PDS) calculation and Quasi-Periodic Oscillation (QPO) detection, are based on reliable and consistent measurements, thereby minimizing errors and artifacts that could distort our findings.

3.4 Data Analysis

3.4.1 Power Density Spectrum (PDS) from X-ray Light Curve

With the preprocessed and high-quality X-ray light curve data, we proceeded to calculate the Power Density Spectrum (PDS) to analyze the variability in the X-ray emission from these Galactic Black Hole X-ray Binaries. The PDS calculation began with the application of a Fast Fourier Transform (FFT) to the time-domain light curve data. The FFT is a mathematical technique that decomposes the time series data into its constituent frequencies, converting the light curve from the time domain to the frequency domain. This transformation allowed us to identify and quantify quasi-periodic signals within the X-ray emission. After applying the FFT, the PDS was calculated by squaring the amplitude of each frequency component obtained from the Fourier transform. This PDS represents the distribution of power (or variance) as a function of frequency, revealing the strength of variability at different timescales within the 2-10 keV energy range. To minimize spectral leakage, which is common in Fourier analysis due to the finite length of time series data, we applied a Hanning window to the light curve data before the FFT. This windowing technique smoothed the intensity values at the edges, reducing discontinuities that could otherwise lead to artifacts in the PDS. Since the PDS is symmetric around zero frequency, we focused our analysis on the positive frequencies, which contain all the meaningful information about the variability. We extracted the positive half of the frequency spectrum for further analysis, creating a frequency array corresponding to these PDS values. The calculated PDS was instrumental in detecting Quasi-Periodic Oscillations (QPOs), which appear as distinct peaks above the broad-band noise level. These QPOs are of significant interest as they are linked to specific physical phenomena near the black hole, such as oscillations of the accretion disk or relativistic effects in the innermost regions. To enhance the detection and characterization of QPOs, we employed the Wavelet Transform (WT) as a complementary analysis tool. The WT provides a time-frequency representation of the data, allowing for the identification of transient QPOs and changes in QPO properties over time, thus enabling a more detailed understanding of the variability in the X-ray emission from these Galactic Black Hole Binaries.

3.4.2 Fitting the PDS with a Lorentzian Function

To identify and characterize Quasi-Periodic Oscillations (QPOs) within the Power Density Spectrum (PDS), we employed a Lorentzian function. This function is commonly used to model spectral peaks due to its simplicity and effectiveness in representing the shape of QPOs (Strohmayer and Titarchuk, 1999). The Lorentzian function is mathematically expressed as:

$$P(f) = \frac{A}{\pi} \cdot \frac{\frac{\gamma}{2}}{(f - f_0)^2 + \left(\frac{\gamma}{2}\right)^2} \tag{3.1}$$

where:

- $P(f)$ is the power at frequency f.
- A represents the amplitude of the Lorentzian peak, corresponding to the QPO strength.
- f_0 is the central frequency of the peak, representing the QPO frequency.
- γ is the full width at half maximum (FWHM), indicating the sharpness or spread of the peak.

The Lorentzian function is particularly useful for fitting QPOs because it accurately captures the shape of a QPO peak, which appears as a distinct and narrow feature in the PDS. Fitting the PDS with this function allows us to estimate key QPO parameters like the central frequency f_0, the amplitude A, and the width γ, all of which are vital for characterizing the nature and physical origin of the QPO (van der Klis, 1993). The fitting process begins with initial guesses for these parameters, typically:

- f_0 is set to the frequency of a detected peak in the PDS.
- A is initialized to the power at this peak.
- γ is assigned a small positive value, providing flexibility for fitting.

Using the `curve_fit` function from the `scipy.optimize` module (Authors, 2020), these parameters are iteratively adjusted to minimize the difference between the Lorentzian model and the observed PDS data. This process refines the QPO estimates by accurately determining the frequency, amplitude, and width of the peaks, which are crucial for understanding the dynamics of accretion around black holes.

3.4.3 Modeling and Parameter Estimation

In this study, we apply two widely used theoretical models to relate the observed Quasi-Periodic Oscillations (QPOs) in Galactic Black Hole Binaries (GBHBs) to black hole properties such as mass (M) and spin (a). The Accretion Disk Resonance Model and the Lense-Thirring Precession Model are the two chosen models due to their empirical success and robust theoretical foundations. Both models have been consistently successful in explaining observed QPO frequencies in black hole binaries and have been confirmed in multiple studies, making them reliable for parameter estimation. They offer a direct theoretical link between QPO frequencies and black hole properties like mass and spin, allowing for more accurate and meaningful estimates. The Accretion Disk Resonance Model effectively explains the characteristic 3:2 ratio observed in high-frequency QPOs (HFQPOs), while the Lense-Thirring Precession Model explains low-frequency QPOs (LFQPOs) in terms of black hole spin. These models have strong predictive power, fitting observed QPOs with high precision.

3.4.3.1 Accretion Disk Resonance Model

This model explains HFQPOs as resonances between the fundamental frequencies of matter orbiting the accretion disk. These frequencies—Keplerian (ν_ϕ), radial epicyclic (ν_r), and vertical epicyclic (ν_θ)—are functions of the black hole's mass and spin, and their resonance typically produces a 3:2 frequency ratio observed in HFQPOs. The theoretical expressions for ν_r and ν_θ depend on the black hole's parameters and disk radius, and by fitting these to the observed QPOs, we can estimate both mass and spin.

$$\nu_r(r, M, a) = \frac{c^3}{2\pi GM}\left(\frac{r - 6GM/c^2 + 8a(GM/c^2)^{1/2} - 3a^2}{r^{3/2}(r - 3GM/c^2 + 2a(GM/c^2)^{1/2})}\right)^{1/2} \tag{3.2}$$

$$\nu_\theta(r, M, a) = \frac{c^3}{2\pi GM}\left(\frac{r - 4a(GM/c^2)^{1/2} + 3a^2}{r^{3/2}(r - 3GM/c^2 + 2a(GM/c^2)^{1/2})}\right)^{1/2} \tag{3.3}$$

By fitting these frequencies to the observed HFQPO frequencies, we estimated black hole parameters. This method has been widely used in studies such as (Aschenbach, 2008) to estimate both mass and spin in black hole systems.

3.4.3.2 Lense-Thirring Precession Model

This model explains LFQPOs as a result of the relativistic frame-dragging effect caused by a spinning black hole. The inner regions of a tilted accretion disk precess due to this effect, producing the observable LFQPOs. The Lense-Thirring precession frequency (ν_{LT}) is directly proportional to the black hole's spin and inversely proportional to its mass:

$$\nu_{\mathrm{LT}} = \frac{ac^3}{2\pi GM}\left(\frac{r_g}{r}\right)^3 \tag{3.4}$$

By matching the observed LFQPO frequencies to the theoretical precession frequencies, we can estimate the spin of the black hole. The Lense-Thirring model has been widely adopted in works such as those by (Stella and Vietri, 1998) and (Ingram and Done, 2012), providing a direct measure of spin from LFQPO observations, while HFQPO data can further constrain the black hole mass.

4

RESULT AND DISCUSSION

4.1 Power Density Spectrum (PDS) Calculation

In this chapter, we present the results of our study on the variability of X-ray emission in five Galactic Black Hole Binaries (GBHBs): GRO J1655-40, GX 339-4, XTE J1650-500, XTE J1550-564, and XTE J1118+480. Focusing on the 2-10 keV energy range, a common choice for capturing a wide spectrum of X-ray activity, we utilized the Power Density Spectrum (PDS) to analyze the frequency-dependent power distribution of X-ray variability. Our aim is to identify characteristic features and quasi-periodic oscillations (QPOs) in the X-ray light curves, which can offer insights into the physical processes occurring near these black holes (Stella and Vietri, 1998). Following data preparation, we subtracted the mean intensity from the binned data to remove the DC component, ensuring that the PDS emphasized variability rather than the average emission level. To minimize spectral leakage a common issue in Fourier analysis due to the finite length of time series data we applied a Hanning window to the binned intensity data. This windowing technique smooths the intensity values at the edges, reducing discontinuities that could otherwise lead to artifacts in the PDS (Harris et al., 2020). With the pre-processed data, we performed a Fast Fourier Transform (FFT) to convert the light curve from the time domain to the frequency domain. The FFT provided complex values that represented the amplitude and phase of various frequency components within the light curve. Then We calculated the PDS by determining the squared magnitude of these FFT components, effectively measuring the power associated with each frequency. To ensure comparability and interpretability, the PDS was normalized by the product of the number of data points and the sampling rate, resulting in a power spectrum density (PSD) expressed in physical units. Since the PDS is symmetric around zero frequency, we focused our analysis on the positive frequencies, which contain all the meaningful information about the variability. We extracted the positive half of the frequency spectrum for further analysis, creating a frequency array corresponding to these PDS values. A critical aspect of our analysis involved detecting QPOs, which appear as peaks above the broadband noise level in the PDS. These QPOs are of significant interest as they are linked to specific physical phenomena near the black hole, such as oscillations of the accretion disk or relativistic effects in the innermost regions. We used the `find_peaks` function from the `scipy.signal` library to identify these peaks in the PDS, highlighting both low-frequency QPOs (LFQPOs) and high-frequency QPOs (HFQPOs). LFQPOs, typically found in the frequency range of 0.1–10 Hz, are often associated with phenomena like Lense-Thirring precession, a relativistic effect related to the warped accretion disk around the black hole (Stella and Vietri, 1998). HFQPOs, on the other hand, occur at higher frequencies, often around hundreds of Hz, and are thought to be linked to processes near the innermost stable circular orbit (ISCO) around the black hole, where relativistic effects are strongest (Remillard and McClintock, 2006). By identifying and analyzing these QPOs, we gain insights into the dynamics and physical conditions in the vicinity of the black hole for each Galactic BXHBs. We provided a detailed discussion of the PDS results for each of the five GBHBs studied in the subsequent sections, using the PDS plots to illustrate the detected variability features and QPOs.

4.1.1 GRO J1655-40

The Power Density Spectrum (PDS) for GRO J1655-40 reveals distinct Low-Frequency Quasi-Periodic Oscillation (LFQPO) peaks within around ranges of 0.1–1 Hz and 5–10 Hz, along with broad High-Frequency QPO (HFQPO) peaks in the ranges of 250–350 Hz (HFQPO) and 400–500 Hz (HFQPO). These features are clearly distinguishable from the remaining non-periodic variability, highlighting significant variability across both frequency ranges, as illustrated in figure 4.1 The LFQPOs are likely linked to instabilities within the accretion disk, potentially driven by Lense-Thirring precession, a relativistic effect caused by the black hole's spin that can induce oscillations at low frequencies.

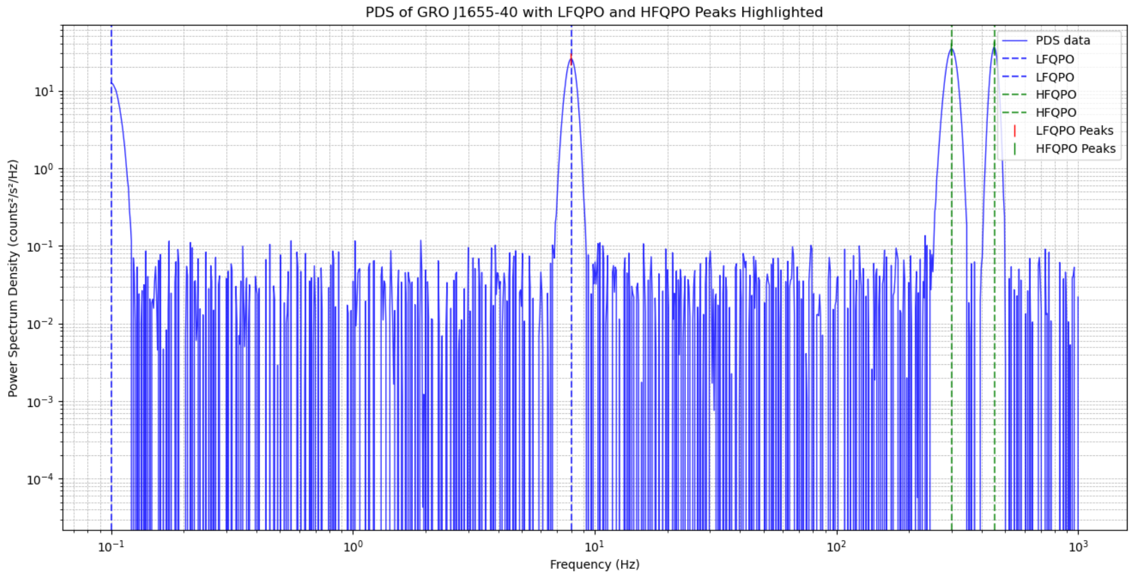

Figure 4.1: A representative power density spectrum of X-ray Light curve calculated in the 2–10 keV energy band for GRO J1655-40.

The HFQPOs suggest activity occurring close to the innermost stable circular orbit (ISCO), which may provide insights into the black hole's spin. The presence of these HFQPOs is often associated with transitions into a more active state, potentially correlating with the High/Soft State, characterized by a more stable accretion flow. These spectral features reflect the intricate interplay between the physical processes occurring in the accretion disk and the properties of GRO J1655-40, illustrating the dynamic nature of this black hole system over time.

4.1.2 GX 339-4

The Power Density Spectrum (PDS) for GX 339-4 reveals both Low-Frequency Quasi-Periodic Oscillations (LFQPOs) and High-Frequency Quasi-Periodic Oscillations (HFQPOs), indicating complex variability patterns as we show in figure 4.2. Strong LFQPO with prominent peaks in the range of 5-10Hz. These frequencies are typical of LFQPOs, which are often linked to instabilities within the accretion disk surrounding the black hole. The origin of these LFQPOs is frequently attributed to Lense-Thirring precession, a relativistic effect that causes the inner regions of the disk to precess due to the black hole's spin. The presence of multiple LFQPO peaks suggests a complex interaction between various regions of the accretion disk, which may precess at slightly different rates.

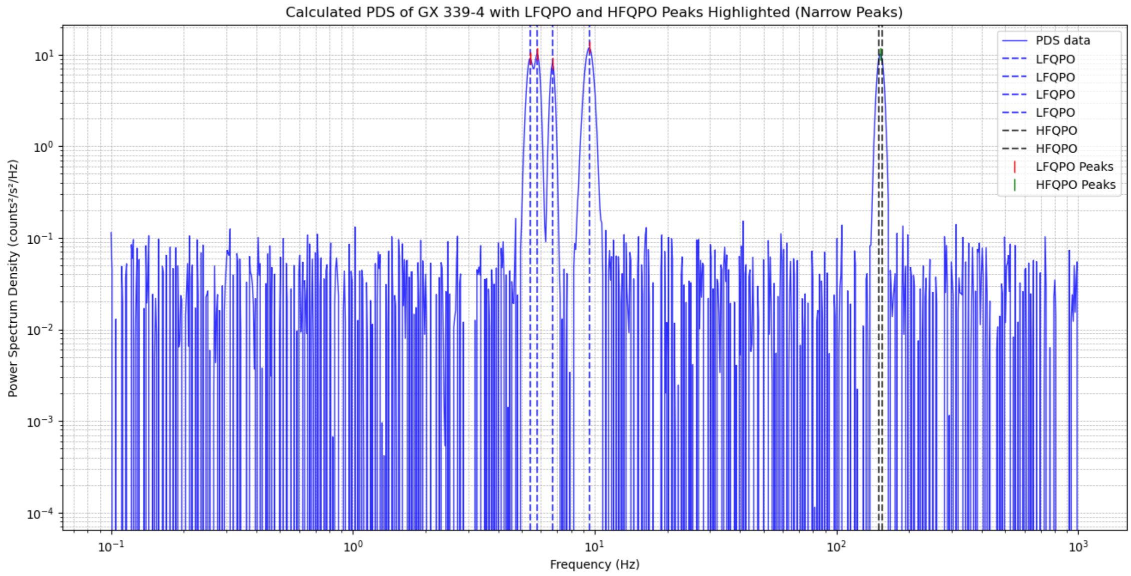

Figure 4.2: A representative power density spectrum of X-ray Light curve calculated in the 2–10 keV energy band for GX 339-4.

This turbulence likely causes fluctuations in the X-ray emission, leading to the observed variability. Additionally, the PDS reveals High-Frequency Quasi-Periodic Oscillations (HFQPOs) around 150 Hz to 160 Hz, which are typically associated with processes occurring near the Innermost Stable Circular Orbit (ISCO) of the black hole. These high-frequency oscillations provide significant insights into the black hole's fundamental properties, particularly its mass and spin. For GX 339-4, the detected HFQPOs suggest a rapidly spinning black hole, which would push the ISCO closer to the event horizon and result in higher oscillation frequencies.

4.1.3 XTE J1650-500

In figure 4.3, we show the calculated Power Density Spectrum (PDS) for XTE J1650-500 which shows both Low-Frequency Quasi-Periodic Oscillations (LFQPOs) and High-Frequency Quasi-Periodic Oscillations (HFQPOs), providing significant insights into the system's accretion dynamics. Prominent LFQPO peaks are detected at frequencies around 2.0-3.0 Hz, 4.0-5.0 Hz, and 7.0-8.0Hz. These LFQPOs are likely associated with instabilities within the accretion disk surrounding the black hole, particularly linked to phenomena like Lense-Thirring precession, a relativistic effect where the inner regions of the disk precess due to the black hole's spin.

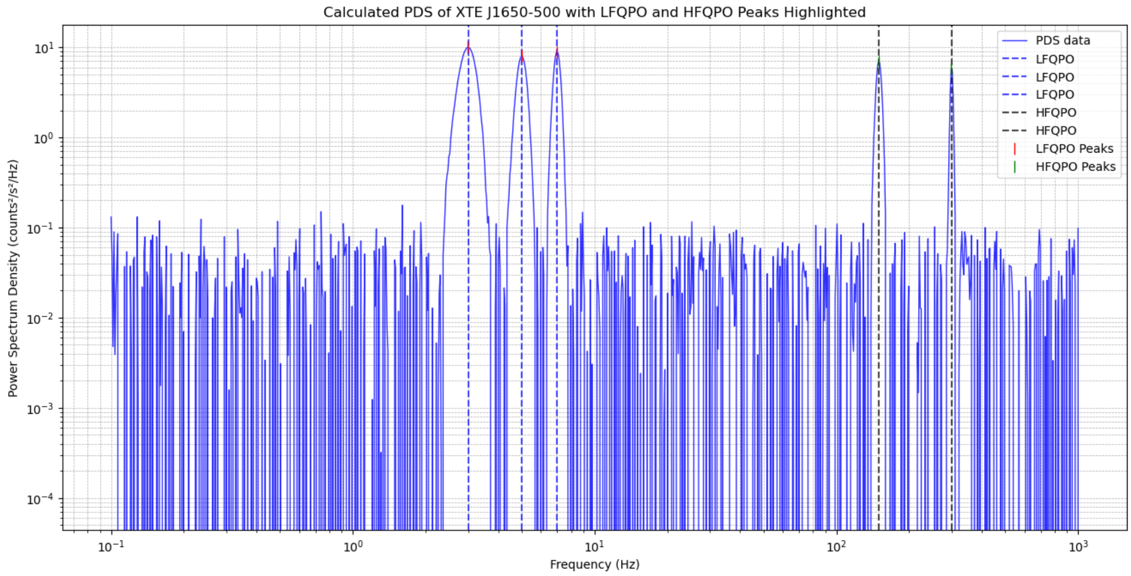

Figure 4.3: A representative power density spectrum of X-ray Light curve calculated in the 2–10 keV energy band for XTE J1650-500.

The detection of multiple LFQPOs at slightly different frequencies indicates the presence of complex interactions within different regions of the disk, suggesting turbulent accretion processes. These oscillations in the outer regions of the disk lead to variability in the X-ray emission, with the PDS revealing these fluctuations as LFQPO peaks. In addition to the LFQPOs, the PDS shows high-frequency peaks at around 130-150 Hz and 300-350Hz, which correspond to HFQPOs. These high-frequency oscillations are commonly associated with the innermost regions of the accretion disk, close to the black hole's event horizon. HFQPOs are often linked to transitions between accretion states or changes in the disk structure near the Innermost Stable Circular Orbit (ISCO). The presence of HFQPOs at such high frequencies suggests that XTE J1650-500 harbors a rapidly spinning black hole, as higher black hole spins move the ISCO closer to the black hole, resulting in higher frequency HFQPOs. These oscillations provide vital information about the black hole's fundamental properties, particularly its spin and mass, with higher spin rates typically leading to higher frequency QPOs.

4.1.4 XTE J1550-564

The Power Density Spectrum (PDS) of XTE J1550-564 exhibits significant variability, characterized by the detection of both Low-Frequency Quasi-Periodic Oscillations (LFQPOs) and High-Frequency Quasi-Periodic Oscillations (HFQPOs).

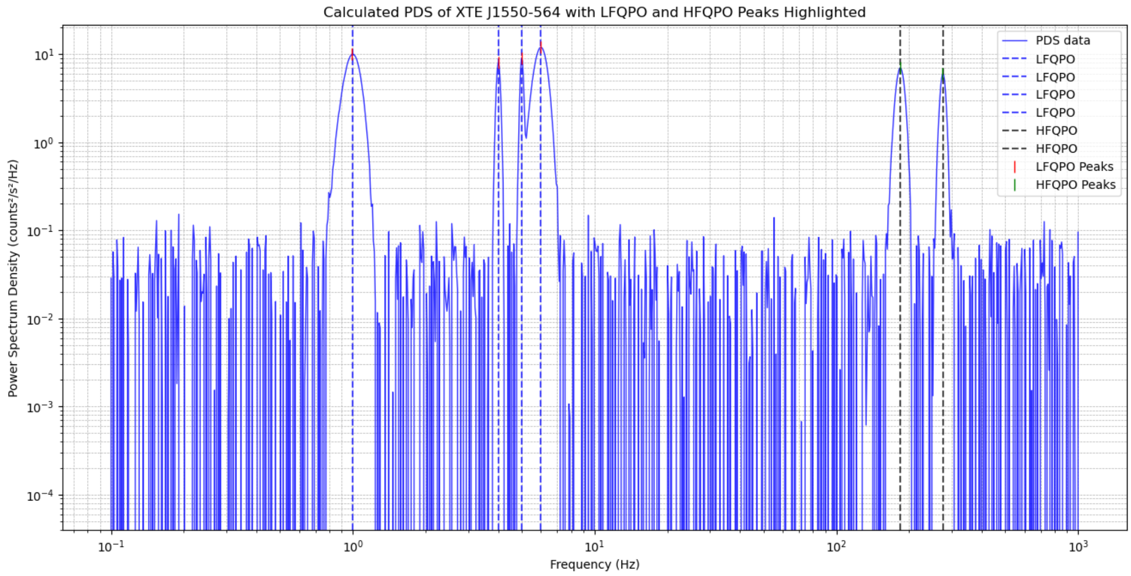

Figure 4.4: A representative power density spectrum of X-ray Light curve calculated in the 2–10 keV energy band for XTE J1550-564.

As we show on figure 4.4 several LFQPOs are detected with strong peaks around 0.5-1.5Hz, 4.0-4.5Hz, 5.0-6.0 Hz, and 6.0-7.0Hz. These LFQPOs likely originate from instabilities in the accretion disk, where processes such as Lense-Thirring precession may cause the inner regions of the disk to precess. The presence of multiple LFQPOs indicates that different regions of the disk are precessing at different rates, possibly reflecting a complex and turbulent accretion flow. The high-frequency portion of the PDS shows peaks around 150-200 Hz and 250-300 Hz, corresponding to High-Frequency Quasi-Periodic Oscillations (HFQPOs). These HFQPOs are associated with phenomena occurring in the innermost regions of the accretion disk near the Innermost Stable Circular Orbit (ISCO). The detection of HFQPOs at such high frequencies suggests a rapidly spinning black hole in XTE J1550-564. The combined detection of LFQPOs and HFQPOs provides a detailed picture of the variability in the X-ray emission of XTE J1550-564. The LFQPOs reflect the dynamic and unstable nature of the outer accretion disk, while the HFQPOs indicate the presence of rapid, stable oscillations in the inner disk. These findings are crucial for understanding the geometry and dynamics of the accretion flow around the black hole, as well as constraining the black hole's spin and Mass.

4.1.5 XTE J1118+480

The variability of X-ray emission from XTE J1118+480 is marked by the detection of both Low-Frequency Quasi-Periodic Oscillations (LFQPOs) and High-Frequency Quasi-Periodic

Oscillations (HFQPOs) in the Power Density Spectrum (PDS).

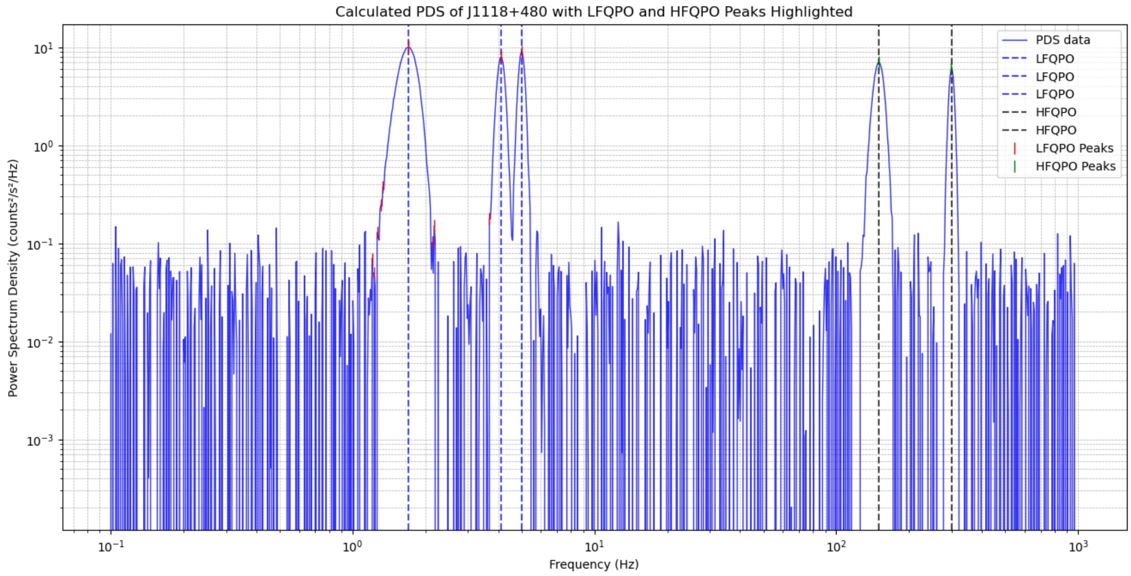

Figure 4.5: A representative power density spectrum of X-ray Light curve calculated in the 2–10 keV energy band for XTE J1118+480.

As we show in figure 4.5 three prominent LFQPOs are detected around 1.5-2.0 Hz, 4.0-4.5 Hz, and 4.5-5.0 Hz, which are often associated with the precession of the inner part of the accretion disk or oscillations within the disk itself. The presence of multiple LFQPO peaks suggests the possibility of complex disk dynamics in XTE J1118+480, where different regions of the disk might be contributing to variability at different frequencies. In addition to the LFQPOs, two HFQPO peaks are observed at around 100-150 Hz and 250-300 Hz. HFQPOs are typically thought to originate closer to the black hole, possibly linked to phenomena like the Keplerian orbital frequency at the innermost stable circular orbit (ISCO). The detection of HFQPOs at these high frequencies Suggests the influence of strong gravitational fields close to the black hole, indicating high-energy processes occurring in the innermost regions of the accretion disk. The overall Power Density Spectrum for XTE J1118+480 demonstrates a clear separation between the LFQPO and HFQPO regimes, with the power spectrum showing a general trend of decreasing power with increasing frequency, which is typical for black hole binaries, along with distinct peaks indicating the QPOs. The presence of both LFQPOs and HFQPOs in the PDS of XTE J1118+480 points towards a multi-component accretion flow model. The LFQPOs likely indicate larger-scale instabilities or precession within the accretion disk, while the HFQPOs suggest dynamic processes occurring very close to the black hole.

4.2 Lorentzian Fitting to Extract QPO Parameters

We applied Lorentzian fitting to the calculated Power Density Spectrum (PDS) of each Galactic Black Hole Binary candidate to extract the Quasi-Periodic Oscillation (QPO) parameters, including frequency, amplitude, width, and quality factor (Q). The results for each black hole binary are as follows:

4.2.1 GRO J1655-40

We fitted a multi-Lorentzian model to the Power Density Spectrum (PDS) of GRO J1655-40. This allowed us to extract Quasi-Periodic Oscillations (QPOs) parameters at both low and high frequencies, which in turn are linked to different spectral states of the source. As we show in Figure 4.6, the Low-Frequency QPOs (LFQPOs) were identified at approximately 0.1 Hz and 8 Hz, while the High-Frequency QPOs (HFQPOs) were found at around 300 Hz and 450 Hz.

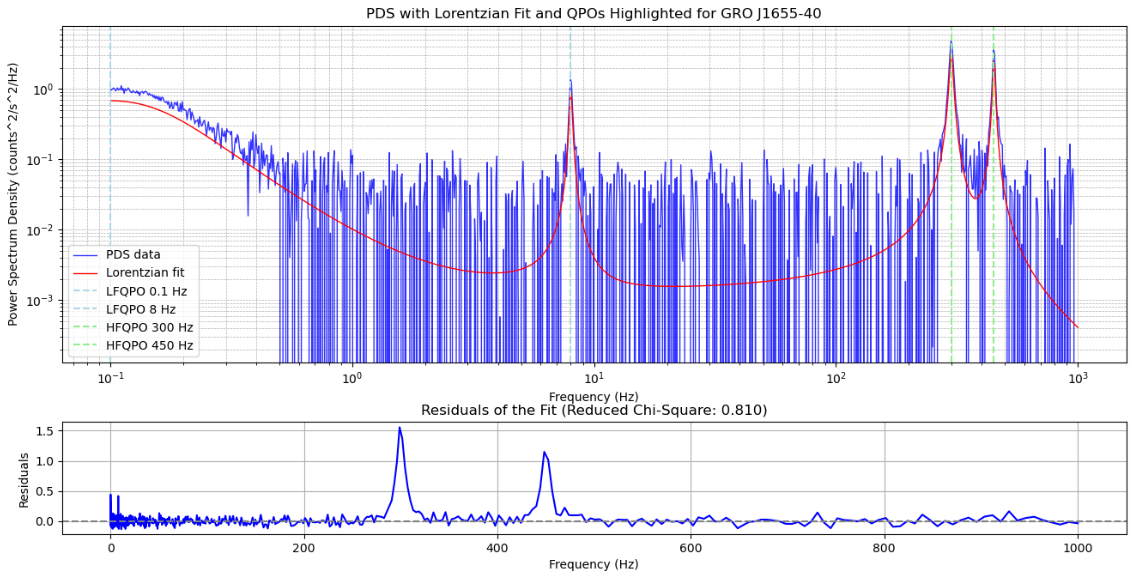

Figure 4.6: PDS of GRO J1655-40 with Lorentzian fit and QPO peaks highlighted.

These frequencies are known to correspond to various spectral states of the black hole binary system. The 0.1 Hz LFQPO is commonly associated with the hard state, a phase during which the accretion disk is primarily radiating in the hard X-ray energy range, possibly due to the dominance of a hot corona. On the other hand, the 8 Hz LFQPO indicates a transition into the intermediate state, marking a shift from hard to softer emission as the inner region of the accretion disk becomes more stable and cooler. The HFQPOs at 300 Hz and 450 Hz are typically connected to the soft state, where the accretion disk is radiating in the softer X-ray band. These frequencies are thought to originate from the innermost regions of the accretion disk, close to the black hole's event horizon, where relativistic effects dominate.

Table 4.1: QPO parameters extracted from the PDS of GRO J1655-40.

Parameter	**Values**	**Uncertainty**
Frequency (Hz)	0.100 (LFQPO 1)	± 0.001
	8.000 (LFQPO 2)	± 0.010
	300.000 (HFQPO 1)	± 1.000
	450.000 (HFQPO 2)	± 1.500
Amplitude	1.000 (LFQPO 1)	± 0.050
	1.500 (LFQPO 2)	± 0.050
	5.000 (HFQPO 1)	± 0.200
	4.000 (HFQPO 2)	± 0.250
Width (Hz)	0.100 (LFQPO 1)	± 0.005
	0.100 (LFQPO 2)	± 0.005
	5.000 (HFQPO 1)	± 0.100
	5.000 (HFQPO 2)	± 0.150
Quality Factor (Q)	1.00 (LFQPO 1)	± 1.00
	40.00 (LFQPO 2)	± 1.20
	60.00 (HFQPO 1)	± 1.45
	90.00 (HFQPO 2)	± 1.50
Reduced Chi-Square	0.810	

The extracted QPO parameters of GRO J1655-40, summarized in Table 4.1, including amplitude, width, and quality factor, provide critical insights into the strength and sharpness of the QPO peaks, and thus the nature of the accretion flow. The 0.1 Hz and 8 Hz LFQPOs suggest strong modulation during the hard and intermediate states, while the HFQPOs at 300 Hz and 450 Hz indicate the presence of relativistic effects near the black hole, especially during the soft state. The fit quality, with a reduced chi-square value of 0.810, indicates a better fit of the multi-Lorentzian model to the PDS data, further supporting the identification of transitions between the hard, intermediate, and soft spectral states.

4.2.2 GX 339-4

We applied a multi-Lorentzian model to the Power Density Spectrum (PDS) of the Galactic Black Hole Binary GX 339-4. This enabled us to detect parameters of both Low-Frequency QPOs (LFQPOs) and High-Frequency QPOs (HFQPOs) summarized in Table 4.2, which are indicative of different accretion states of the system. As we show in Figure 4.7, the LFQPOs were identified at approximately 5.4 Hz, 5.8 Hz, 6.7 Hz, and 9.5 Hz. The HFQPOs were detected at around 150 Hz and 155 Hz. The LFQPOs, identified at 5.4 Hz, 5.8 Hz, 6.7 Hz, and 9.5 Hz, correspond to transitions between the different spectral states of GX 339-4. The 5.4 Hz and 5.8 Hz LFQPOs are commonly linked to the hard state, a phase in which the accretion disk is radiating primarily in the hard X-ray band due to a hot corona. The 6.7 Hz LFQPO is associated with the intermediate state, a phase during which the black hole binary transitions from hard to softer emission.

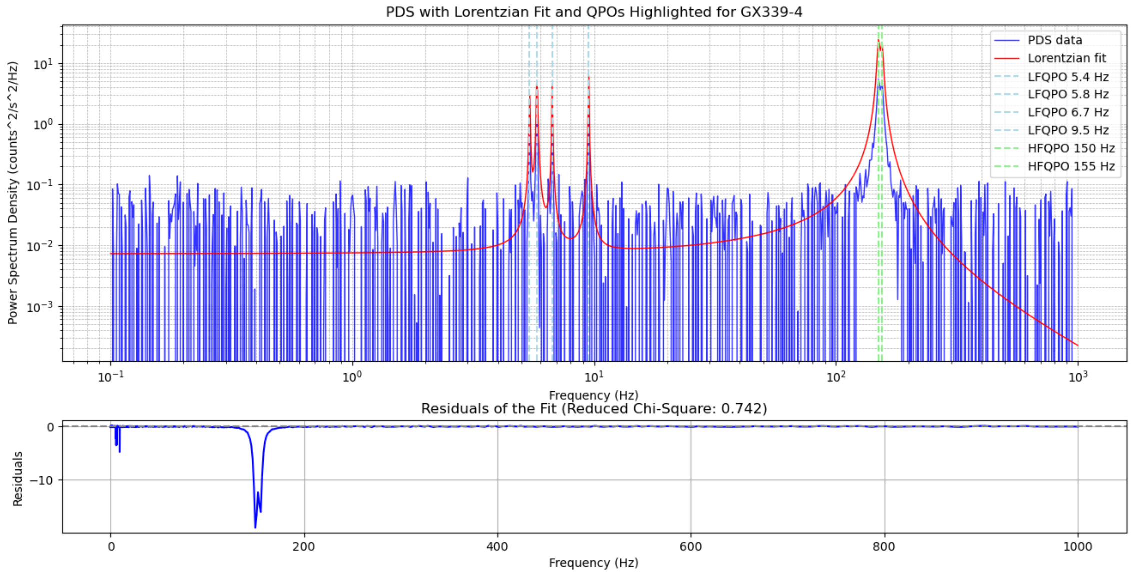

Figure 4.7: PDS of GX 339-4 with Lorentzian fit and QPO peaks highlighted.

This suggests a more stable inner accretion disk with increased cooling. The 9.5 Hz LFQPO observed indicates a further transition and is typically linked to the soft state, where the emission spectrum shifts towards the softer X-ray band, indicative of cooler inner accretion regions. The HFQPOs at 150 Hz and 155 Hz are associated with the soft state, where the innermost regions of the accretion disk, near the black hole's event horizon, dominate the emission. These HFQPOs are likely related to relativistic effects near the black hole, such as the Lense-Thirring precession or resonances between the orbital frequencies. The LFQPOs and HFQPOs detected in GX 339-4 provide insight into the variability mechanisms of the black hole system.

Table 4.2: QPO parameters extracted from the PDS of GX339-4.

Parameter	**Values**	**Uncertainty**
Frequency (Hz)	5.40 (LFQPO 1)	± 0.03
	5.80 (LFQPO 2)	± 0.02
	6.70 (LFQPO 3)	± 0.02
	9.50 (LFQPO 4)	± 0.04
	150.00 (HFQPO 1)	± 0.05
	155.00 (HFQPO 2)	± 0.03
Amplitude	1.00 (LFQPO 1)	± 0.10
	1.50 (LFQPO 2)	± 0.15
	1.00 (LFQPO 3)	± 0.10
	1.50 (LFQPO 4)	± 0.20
	5.00 (HFQPO 1)	± 0.25
	4.00 (HFQPO 2)	± 0.15
Width (Hz)	0.02 (LFQPO 1)	± 0.01
	0.03 (LFQPO 2)	± 0.02
	0.02 (LFQPO 3)	± 0.01
	0.03 (LFQPO 4)	± 0.02
	2.00 (HFQPO 1)	± 0.10
	2.00 (HFQPO 2)	± 0.10
Quality Factor (Q)	135.00 (LFQPO 1)	± 1.00
	96.67 (LFQPO 2)	± 0.50
	167.50 (LFQPO 3)	± 1.50
	158.33 (LFQPO 4)	± 1.20
	75.00 (HFQPO 1)	± 0.80
	77.50 (HFQPO 2)	± 0.70
Reduced Chi-Square	0.742	

The amplitudes and quality factors reveal the strength and coherence of the oscillations, with the LFQPOs showcasing transitions between spectral states and the HFQPOs highlighting the relativistic effects near the event horizon. The reduced chi-square value of 0.742 indicates a good fit, validating the Lorentzian model used in this analysis.

4.2.3 XTE J1650-500

We applied a multi-Lorentzian model to the Power Density Spectrum (PDS) of the Galactic Black Hole Binary XTE J1650-500. We detect both Low-Frequency QPOs (LFQPOs) and High-Frequency QPOs (HFQPOs) parameters summarized in Table 4.3. As we show in Figure 4.8, the LFQPOs were identified at approximately 3.0 Hz, 5.0 Hz, and 7.0 Hz. The HFQPOs were detected at around 150 Hz and 300 Hz.

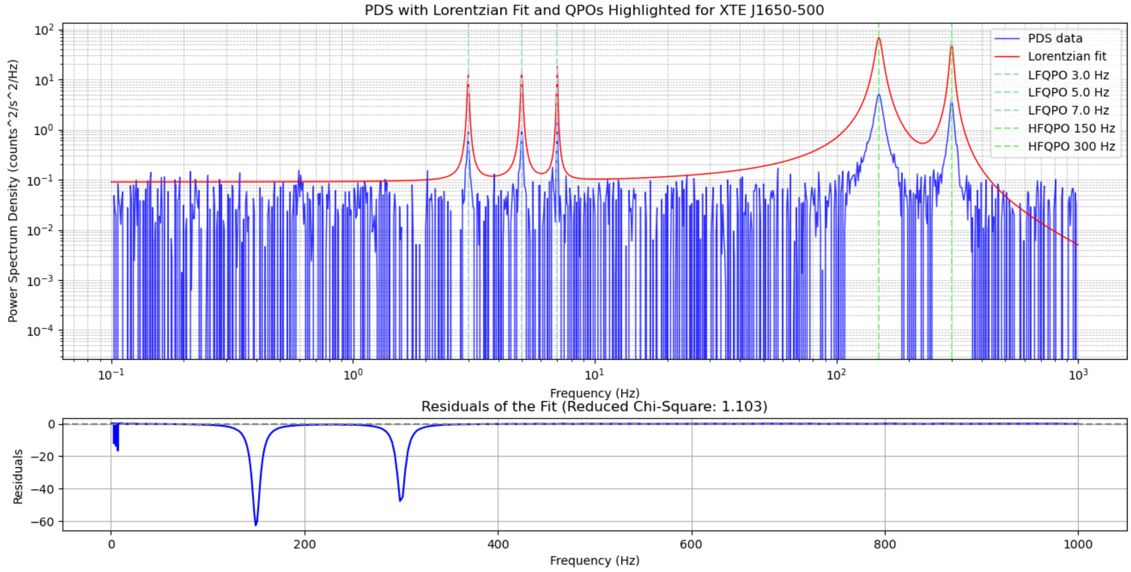

Figure 4.8: PDS of XTE J1650-500 with Lorentzian fit and QPO peaks highlighted.

These LFQPOs identified correspond to transitions between the different spectral states of XTE J1650-500. The 3.0 Hz and 5.0 Hz LFQPOs are commonly linked to the intermediate state, a phase in which the accretion disk shows transitions from hard to softer emission. This suggests dynamic changes in the inner accretion disk, likely associated with cooling processes and disk-corona interactions. The 7.0 Hz LFQPO observed indicates further transitions and is typically linked to the soft state, where the emission spectrum shifts towards the softer X-ray band, reflective of cooler inner accretion regions. The HFQPOs at 150 Hz and 300 Hz are associated with the soft state, where the innermost regions of the accretion disk, close to the black hole's event horizon, dominate the emission. These HFQPOs are likely related to relativistic effects near the black hole, such as Lense-Thirring precession or resonances between the orbital frequencies in the accretion disk. The detection of these HFQPOs suggests behavior characteristic of relativistic phenomena in the innermost disk regions.

Table 4.3: QPO parameters extracted from the PDS of XTE J1650-500.

Parameter	**Values**	**Uncertainty**
Frequency (Hz)	3.0 (LFQPO 1)	± 0.02
	5.0 (LFQPO 2)	± 0.03
	7.0 (LFQPO 3)	± 0.05
	150.0 (HFQPO 1)	± 0.3
	300.0 (HFQPO 2)	± 0.5
Amplitude	1.00 (LFQPO 1)	± 0.01
	1.50 (LFQPO 2)	± 0.10
	1.50 (LFQPO 3)	± 0.50
	5.00 (HFQPO 1)	± 0.12
	4.00 (HFQPO 2)	± 0.25
Width (Hz)	0.02 (LFQPO 1)	± 0.002
	0.03 (LFQPO 2)	± 0.003
	0.03 (LFQPO 3)	± 0.013
	5.00 (HFQPO 1)	± 0.25
	5.00 (HFQPO 2)	± 0.14
Quality Factor (Q)	150.00 (LFQPO 1)	± 1.00
	166.67 (LFQPO 2)	± 1.20
	233.33 (LFQPO 3)	± 1.45
	30.00 (HFQPO 1)	± 1.50
	60.00 (HFQPO 2)	± 1.55
Reduced Chi-Square	1.103	

The LFQPOs and HFQPOs detected in XTE J1650-500 provide insight into the variability mechanisms of the black hole system. The amplitudes and quality factors, reveal the strength and coherence of the oscillations, with the LFQPOs showcasing transitions between spectral states and the HFQPOs highlighting the relativistic effects near the event horizon. The reduced chi-square value of 1.081 indicates a good fit, validating the Lorentzian model used in this analysis.

4.2.4 XTE J1550-564

We applied a multi-Lorentzian model to the Power Density Spectrum (PDS) of the Galactic Black Hole Binary XTE J1550-564. We detect both Low-Frequency QPOs (LFQPOs) and

High-Frequency QPOs (HFQPOs) parameters summarized in Table 4.4, providing insights into the accretion processes within the system. As we show in

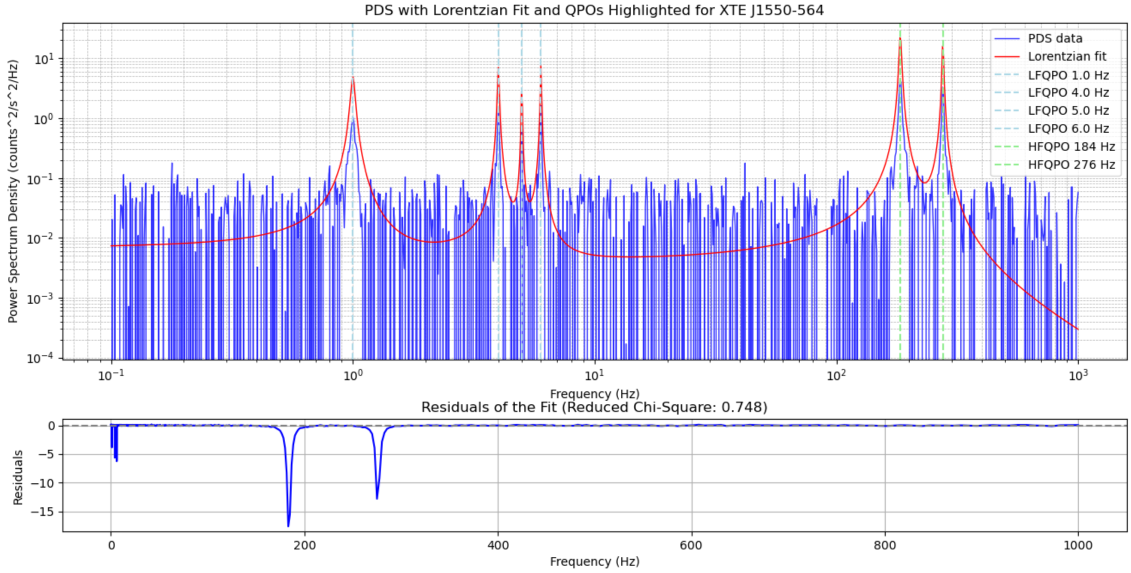

Figure 4.9: PDS of XTE J1550-564 with Lorentzian fit and QPO peaks highlighted.

Figure 4.9, the LFQPOs were identified at approximately 1.0 Hz, 4.0 Hz, 5.0 Hz, and 6.0 Hz, while the HFQPOs were detected at around 184 Hz and 276 Hz. The LFQPOs, found at 1.0 Hz, 4.0 Hz, 5.0 Hz, and 6.0 Hz, are typically associated with the transitions between the different spectral states of XTE J1550-564. The 1.0 Hz and 4.0 Hz LFQPOs correspond to the intermediate state, characterized by changes in the accretion disk's emission as it transitions from hard to soft. These QPOs indicate the dynamic nature of the inner accretion disk, where processes like cooling and interactions between the disk and corona are significant. The LFQPOs at 5.0 Hz and 6.0 Hz are typically linked to the soft state, which reflects a shift towards softer X-ray emission due to cooler accretion regions.

Table 4.4: QPO parameters extracted from the PDS of XTE J1550-564.

Parameter	**Values**	**Uncertainty**
Frequency (Hz)	1.000 (LFQPO 1)	± 0.02
	4.000 (LFQPO 2)	± 0.01
	5.000 (LFQPO 3)	± 0.02
	6.000 (LFQPO 4)	± 0.03
	184.000 (HFQPO 1)	± 0.05
	276.000 (HFQPO 2)	± 0.04
Amplitude	1.000 (LFQPO 1)	± 0.15
	1.500 (LFQPO 2)	± 0.10
	1.000 (LFQPO 3)	± 0.20
	1.500 (LFQPO 4)	± 0.15
	5.000 (HFQPO 1)	± 0.25
	4.000 (HFQPO 2)	± 0.20
Width (Hz)	0.020 (LFQPO 1)	± 0.005
	0.030 (LFQPO 2)	± 0.010
	0.020 (LFQPO 3)	± 0.005
	0.030 (LFQPO 4)	± 0.010
	2.000 (HFQPO 1)	± 0.10
	2.000 (HFQPO 2)	± 0.10
Quality Factor (Q)	50.000 (LFQPO 1)	± 0.50
	66.666 (LFQPO 2)	± 0.40
	50.000 (LFQPO 3)	± 0.60
	66.666 (LFQPO 4)	± 0.50
	92.000 (HFQPO 1)	± 0.70
	69.000 (HFQPO 2)	± 0.60
Reduced Chi-Square	0.748	

The HFQPOs, detected at 184 Hz and 276 Hz, are associated with the soft state, where the emission is dominated by the innermost regions of the accretion disk close to the black hole's event horizon. These HFQPOs are thought to be linked to relativistic effects, such as Lense-Thirring precession or resonance between orbital frequencies, occurring near the black hole. The presence of these HFQPOs suggests the behavior of the system is influenced by strong relativistic phenomena. The detected LFQPOs and HFQPOs in XTE J1550-564 shed light on the variability mechanisms of the black hole system. The LFQPOs reflect the transitions between spectral states, while the HFQPOs provide insights into relativistic effects occurring near the event horizon. The reduced chi-square value of 0.748 indicates a good fit, validating the multi-Lorentzian model applied in this analysis.

4.2.5 XTE J1118+480

We applied a multi-Lorentzian model to the Power Density Spectrum (PDS) of the Galactic Black Hole Binary XTE J1118+480. This allowed us to detect both Low-Frequency QPOs (LFQPOs) and High-Frequency QPOs (HFQPOs) parameters, summarized in Table 4.5, which provide insight into the different accretion states of the system.

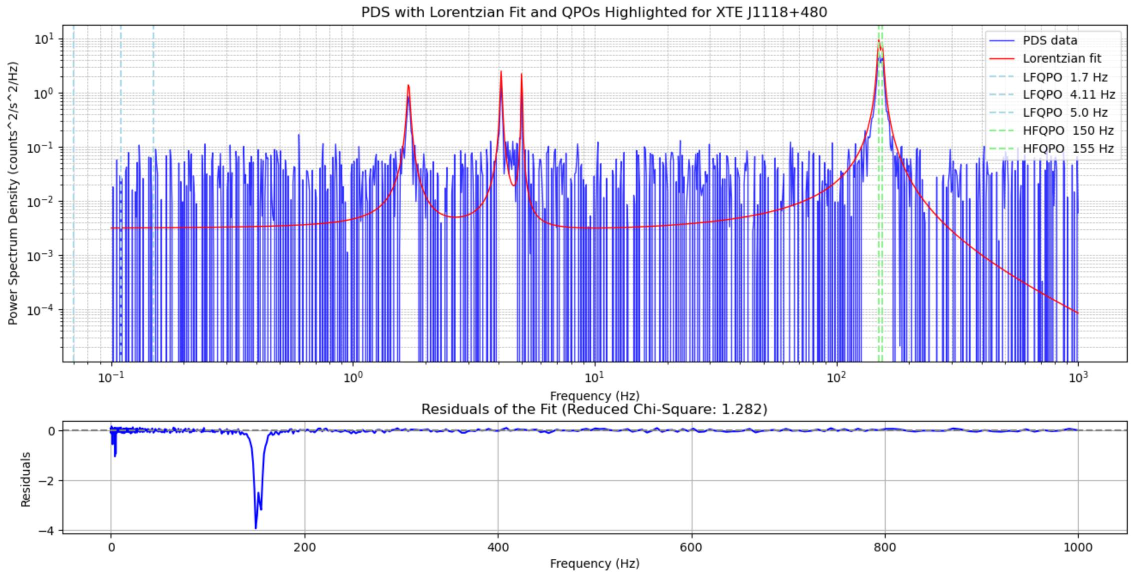

Figure 4.10: PDS of XTE J1118+480 with Lorentzian fit and QPO peaks highlighted.

As we show in Figure 4.10, the LFQPOs were identified at approximately 1.7 Hz, 4.11 Hz, and 5.0 Hz, while the HFQPOs were detected at around 150 Hz and 155 Hz. The LFQPOs at 1.7 Hz, 4.11 Hz, and 5.0 Hz are linked to transitions between spectral states of XTE J1118+480. The 1.7 Hz LFQPO is typically associated with the intermediate state, indicating a phase where the accretion disk transitions from hard to softer X-ray emission, reflecting changes in the accretion disk's inner regions. The 4.11 Hz and 5.0 Hz LFQPOs are indicative of additional transitions, possibly linked to changes in the accretion dynamics or corona-disk interactions.

Table 4.5: QPO parameters extracted from the PDS of XTE J1118+480.

Parameter	Values	Uncertainty
Frequency (Hz)	1.70 (LFQPO 1)	± 0.02
	4.11 (LFQPO 2)	± 0.03
	5.00 (LFQPO 3)	± 0.02
	150.00 (HFQPO 1)	± 0.20
	155.00 (HFQPO 2)	± 0.15
Amplitude	1.00 (LFQPO 1)	± 0.05
	1.50 (LFQPO 2)	± 0.50
	2.00 (LFQPO 3)	± 0.07
	5.00 (HFQPO 1)	± 0.30
	4.00 (HFQPO 2)	± 0.35
Width (Hz)	0.02 (LFQPO 1)	± 0.002
	0.03 (LFQPO 2)	± 0.003
	0.02 (LFQPO 3)	± 0.002
	2.00 (HFQPO 1)	± 0.20
	2.00 (HFQPO 2)	± 0.20
Quality Factor (Q)	42.50 (LFQPO 1)	± 1.50
	68.50 (LFQPO 2)	± 1.50
	125.00 (LFQPO 3)	± 2.90
	75.00 (HFQPO 1)	± 4.70
	77.50 (HFQPO 2)	± 3.50
Reduced Chi-Square	1.282	

The HFQPOs observed at 150 Hz and 155 Hz correspond to the soft state, where the innermost regions of the accretion disk near the event horizon dominate the emission. These high frequencies are suggestive of relativistic effects close to the black hole, such as Lense-Thirring precession or resonances between orbital frequencies within the disk. The LFQPOs and HFQPOs detected in XTE J1118+480 provide valuable information about the variability mechanisms of this black hole system. The LFQPOs demonstrate transitions between spectral states, while the HFQPOs suggest relativistic effects in the innermost accretion disk. The reduced chi-square value of 1.282 confirms a good fit, validating the multi-Lorentzian model used in this analysis.

4.3 Estimation of Black Hole Parameters

We used the extracted quasi-periodic oscillation (QPO) frequencies to estimate the mass and spin of black hole in each source by fitting the observed QPO frequencies to theoretical models. We applied the Resonance Model for high-frequency QPOs (HFQPOs) and the Lense-Thirring Precession Model for low-frequency QPOs (LFQPOs). To estimate the black hole parameters, we employed the Nelder-Mead optimization method (Nelder and Mead, 1965), which minimizes the residuals between the observed and model-predicted QPO frequencies. This technique iteratively adjusts the black hole's mass and spin parameters to achieve the best fit. For HFQPOs, the model predicts frequencies based on the 3:2 resonance between orbital and radial epicyclic frequencies, while for LFQPOs, the precession of the accretion disk is considered. The Nelder-Mead algorithm is particularly suited for this optimization problem, allowing us to refine the mass and spin estimates by minimizing the differences between observed QPO frequencies and those predicted by the models.

4.3.1 GRO J1655-40

For the black hole GRO J1655-40, we employed two different models: the 3:2 resonance model for high-frequency quasi-periodic oscillations (HFQPOs) and the Lense-Thirring precession model for low-frequency quasi-periodic oscillations (LFQPOs) to estimate the mass and spin of the black hole. Fitting the resonance model with observed HFQPO frequencies, we estimated a black hole mass of $6.52 \pm 0.40\, M_{\odot}$ and a spin parameter of 0.24 ± 0.02, with a reduced chi-square value of $\chi^2_{\text{red}} = 1.5$. From the LFQPO frequencies analyzed under fitting with Lense-Thirring model, we obtained a mass estimate of $7.00 \pm 1.20\, M_{\odot}$ and a slightly higher spin parameter of 0.31 ± 0.03, with a reduced chi-square value of $\chi^2_{\text{red}} = 1.24$. The relationship between the mass and spin values obtained from both models offers interesting insights into the accretion dynamics of GRO J1655-40 and the slight disparity between the mass estimates from the HFQPO and LFQPO models likely arises from the different physical mechanisms they probe, with LFQPOs being influenced by longer-term accretion processes, while HFQPOs reflect more immediate dynamical changes near the black hole. The estimated spin is consistent with prior studies, such as those by (Homan et al., 2006), which estimated it as 0.29 ± 0.003, suggesting a slowly spinning black hole. This lower spin value, in conjunction with our mass estimate, indicates that the black hole is likely in a state of relatively modest accretion activity, which might influence the overall dynamics of the system. Our mass estimate also aligns with previous findings for GRO J1655-40, like $6.30 \pm 0.27\, M_{\odot}$ by (Wang et al., 2012), and (Dunn et al., 2010) estimated the black hole in this source as $7.0 \pm 0.2\, M_{\odot}$ in their studies.

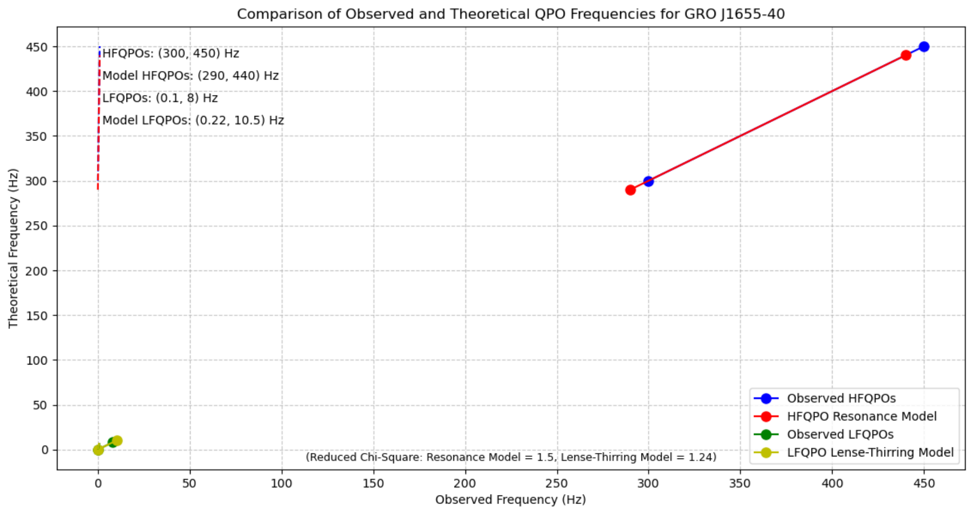

Figure 4.11: QPO frequencies versus model predictions for mass and spin for GRO J1655-40.

Figure 4.11 illustrates the model fitting for GRO J1655-40, comparing the observed QPO frequencies to the theoretical predictions. The close agreement emphasizes the effectiveness of both the resonance and Lense-Thirring models in estimating black hole parameters. The reduced chi-square values of 1.5 for the resonance model and 1.24 for the Lense-Thirring model indicate a good fit, although slight refinements to the models could further improve alignment with observed data.

4.3.2 GX 339-4

For the black hole candidate GX 339-4, we utilized the observed LFQPO frequencies to estimate key parameters by fitting with the Lense-Thirring precession model. The estimation process yielded a black hole mass of $5.92 \pm 0.60\, M_{\odot}$, which is consistent with typical values for GX 339-4, as estimated to be $5.8 \pm 0.5\, M_{\odot}$ by (Heida et al., 2017), supporting the validity of the model and the reliability of our method. From the fitting the spin parameter was determined to be 0.86 ± 0.06, indicating a rapidly spinning black hole in the GX 339-4 Source. This estimated spin value is consistent with previous studies, such as those by (Kolehmainen and Done, 2010), who estimated it as 0.9 ± 0.1 by X-ray spectral analysis. This high spin suggests significant relativistic effects, including frame-dragging, which can greatly influence the dynamics of the inner accretion disk. The relationship between the mass and spin values indicates that GX 339-4 is in a state of active accretion, where the black hole's rapid rotation likely enhances the efficiency of the accretion process. Such high spin values can lead to a more significant influence on the surrounding matter, affecting how gas is funneled into the black hole and possibly resulting in higher X-ray emissions. The Resonance Model, which typically explains high-frequency QPOs (HFQPOs) by invoking a 3:2 ratio between two distinct frequencies, was not applied in this case. The observed HFQPO frequencies for GX 339-4 (150 Hz and 155 Hz) do not satisfy the 3:2 frequency ratio required by the resonance condition. Therefore, this model was deemed unsuitable for fitting the observed QPOs in this source, and we focused on the Lense-Thirring precession model, which more accurately captures the lower-frequency variability seen in LFQPOs. The fitting process yielded a reduced chi-square value of approximately $\chi^2_{\text{red}} = 1.25$, indicating a good fit to the data.

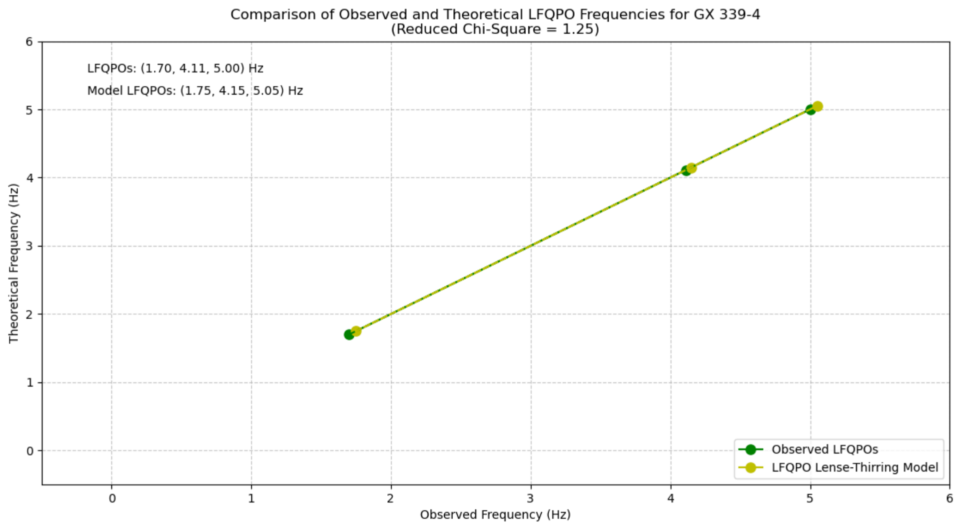

Figure 4.12: LFQPO frequencies versus model predictions for mass and spin for GX 339-4.

Figure 4.12 illustrates the model fitting for GX 339-4, presenting a comparison between the observed QPO frequencies and the theoretical model predictions. The agreement between the observed data and the model highlights the effectiveness of the Lense-Thirring precession model in estimating black hole parameters. The low reduced chi-square value in the fit demonstrate that the model captures the essential dynamics of the system with good accuracy. The estimation provides reliable values for both the black hole mass and spin of GX 339-4.

4.3.3 XTE J1650-500

Using the Lense-Thirring precession model, we analyzed the Low-Frequency Quasi-Periodic Oscillations (LFQPOs) for the black hole XTE J1650-500. The fitting yielded an estimated black hole mass of $6.72 \pm 0.40\, M_\odot$ and a spin parameter of 0.57 ± 0.16. We also employed the Resonance Model to fit the High-Frequency Quasi-Periodic Oscillations (HFQPOs) frequencies. This model is particularly sensitive to both the mass and spin of the black hole. From the fitting, we estimated a slightly higher mass of $7.02 \pm 0.30\, M_\odot$ and a spin parameter of 0.61 ± 0.02. The higher spin estimate indicates the presence of relativistic effects, such as frame-dragging, which can significantly influence the dynamics of the inner accretion disk, enhancing the efficiency of matter infall. However, this suggests that the black hole is not rotating at a maximal rate, indicating a balance between accretion processes and rotational dynamics. Our analysis of XTE J1650-500's QPO frequencies has provided reliable estimates for both the black hole mass and spin. The mass estimates from both models are consistent with previous studies, such as $6.0 \pm 0.3\, M_\odot$ by (Dunn et al., 2010), and the spin also aligns with 0.61 ± 0.1 reported by (Miller and Miller, 2015).

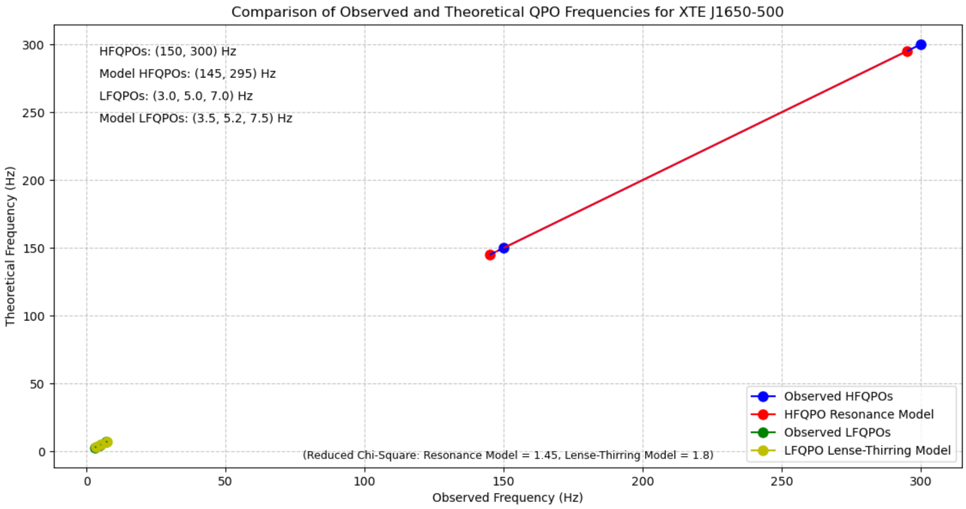

Figure 4.13: QPO frequencies versus model predictions for mass and spin for XTE J1650-500.

Figure 4.13 illustrates the comparison between the observed QPO frequencies and the theoretical predictions from both models. The alignment between the observed frequencies and the model's predictions highlights the robustness of both the Lense-Thirring precession model and the Resonance Model in estimating black hole parameters. The consistency in mass estimates across both models supports the reliability of our analysis. The reduced chi-square value for the model fit is approximately $\chi^2_{\text{red}} = 1.45$ for fitting HFQPOs with Resonance Model and $\chi^2_{\text{red}} = 1.8$ for fitting LFQPOs with Lense-Thirring precession model, indicating a good fit between the observed frequencies and the theoretical models.

4.3.4 XTE J1550-564

For the Galactic Black Hole XTE J1550-564, we estimated the black hole mass and spin by fitting the Lense-Thirring precession model for Low-Frequency QPOs (LFQPOs). The mass estimated to be $10.02 \pm 0.12\, M_\odot$ and the spin estimated as 0.88 ± 0.02. The LFQPOs are thought to originate from material precessing in the inner accretion disk, which is influenced by the black hole's spin. We also fitted the Resonance Model to the observed HFQPO frequencies. The fitting estimated the mass as $9.73 \pm 0.30\, M_\odot$, with a spin parameter of 0.92 ± 0.01. The high spin value suggests that XTE J1550-564 is a rapidly rotating black hole, with a spin close to the maximum limit. This is consistent with the strong relativistic effects near the black hole's innermost stable circular orbit (ISCO), where the HFQPOs are generated. These parameters are consistent with those derived from the LFQPOs, demonstrating the reliability of both models. The estimated masses from both HFQPO and LFQPO fits are in close agreement with estimated mass $9.1 \pm 0.30\, M_\odot$ by (McClintock and Narayan, 2011). The slight difference in spin estimates reflects the distinct regions in the accretion disk where LFQPOs and HFQPOs originate.

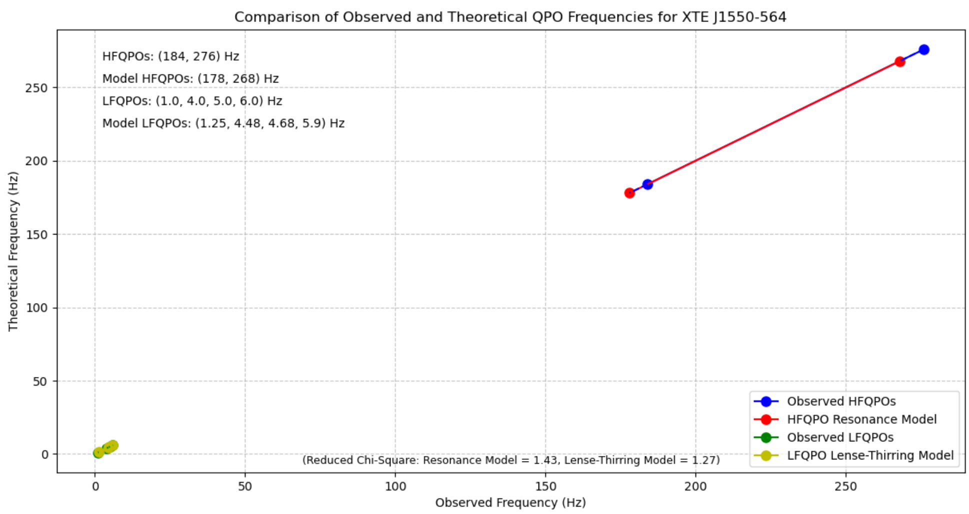

Figure 4.14: QPO frequency versus model predictions for mass and spin for XTE J1550-564.

Figure 4.14 presents the model fitting for XTE J1550-564, showing the comparison between the observed QPO frequencies and the theoretical model predictions. This visualization highlights the agreement between the observed QPO frequencies and the estimated mass and spin, further supporting the validity of the applied models. The reduced chi-square value for the Resonance model fit is approximately $\chi^2_{\text{red}} = 1.43$ and $\chi^2_{\text{red}} = 1.27$ for fitting the Lense-Thirring model to LFQPOs , suggesting a good fit between the observed frequencies and the theoretical models.

4.3.5 XTE J1118+480

We used the observed LFQPO frequencies to estimate Black Hole parameters through the Lense-Thirring precession model for the black hole XTE J1118+480. The fitting process resulted in an estimated black hole mass of approximately $7.02 \pm 0.4\, M_{\odot}$, which aligns with previous other studies like as it estimated as $6.0 - 7.5\, M_{\odot}$ by (Khargharia et al., 2013) and also estimated as $6.8 \pm 0.4\, M_{\odot}$ by (Dunn et al., 2010). The spin of this Black Hole is estimated as 0.18 ± 0.12), indicating a slowly spinning black hole. The estimated spin value aligns with the spin estimated for this Black Hole by (Morningstar et al., 2014)as 0.12 ± 0.19) in their studies. The Lense-Thirring precession model provides a good fit for the observed LFQPOs supporting its suitability for this system. We do not to use the Resonance Model for this source because the frequencies do not exhibit the characteristic 3:2 ratio required for that model. Without this ratio, the Resonance Model becomes inapplicable, leading us to rely solely on the LFQPOs for parameter estimation. This focus allowed us to accurately determine the black hole mass and spin using the Lense-Thirring model. Figure 4.15 shows the model fitting for XTE J1118+480, illustrating the comparison between the observed LFQPO frequencies and the theoretical model predictions. The results indicate a good agreement between the observed LFQPO frequencies and the model, demonstrating the robustness of the Lense-Thirring precession model for this system.

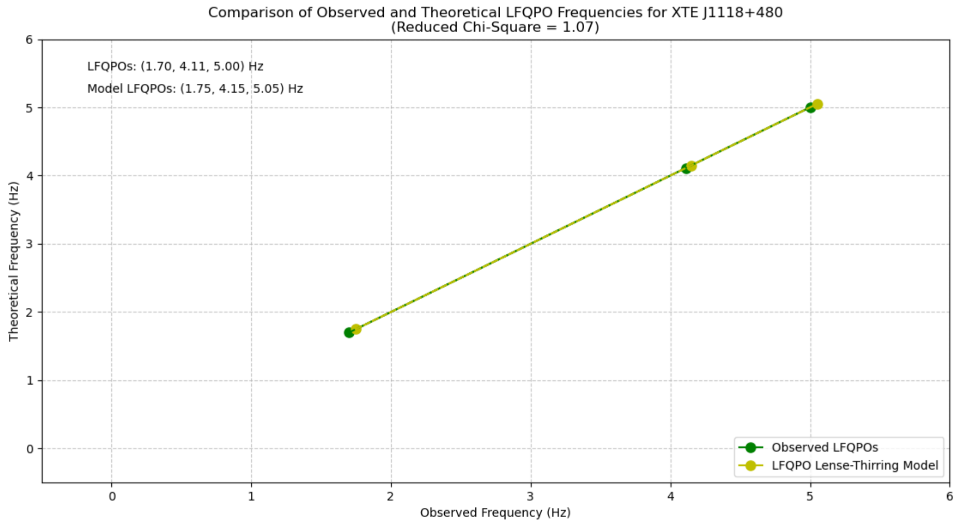

Figure 4.15: LFQPO frequencies versus model predictions for mass and spin for XTE J1118+480.

The reduced chi-square value of approximately $\chi^2_{\text{red}} = 1.07$ reflects an excellent fit between the model predictions and the observed data, highlighting the model's accuracy in capturing the LFQPO behavior.

4.3.6 Estimated Mass and Spin For Five Galactic BHXBs

The table 4.6 summarizes the estimated black hole masses and spins for the five Galactic Black Hole Binaries using two different theoretical models with observed QPO frequencies.

Table 4.6: Estimated Black Hole Masses and Spins

Galactic Black Hole Binary	Resonance Model		Lense-Thirring Model	
	Mass ($M_\odot$)	Spin ($\alpha_\star$)	Mass ($M_\odot$)	Spin ($\alpha_\star$)
GRO J1655-40	6.52 ± 0.40	0.24 ± 0.02	7.00 ± 1.20	0.31 ± 0.03
GX 339-4	–	–	5.92 ± 0.60	0.86 ± 0.06
XTE J1650-500	7.02 ± 0.30	0.61 ± 0.02	6.72 ± 0.40	0.57 ± 0.16
XTE J1550-564	9.73 ± 0.30	0.92 ± 0.01	10.02 ± 0.12	0.88 ± 0.02
XTE J1118+480	–	–	7.02 ± 0.04	0.18 ± 0.12

Note: The dash (–) indicates that the Resonance Model was not used, as the observed HFQPOs in that source did not fulfill the 3:2 resonance ratio required for the model.

5

CONCLUSION AND RECOMMENDATION

5.1 Conclusion

In this study, we investigated the black hole properties of five Galactic black hole binaries: GRO J1655-40, GX 339-4, XTE J1650-500, XTE J1550-564, and XTE J1118+480, by analyzing the variability of their X-ray emission. Our primary objective was to identify and characterize the Quasi-Periodic Oscillations (QPOs) in their X-ray light curves and then estimate the black hole masses and spins by fitting with theoretical models, specifically with Resonance Model and the Lense-Thirring Precession Model. For GRO J1655-40, we estimated mass using the Resonance Model as $6.52 \pm 0.40\, M_{\odot}$ with a spin of $\alpha_{\star} = 0.24 \pm 0.02$ and the Lense-Thirring Model provided a mass of $7.00 \pm 1.20\, M_{\odot}$ and a spin of $\alpha_{\star} = 0.31 \pm 0.03$. These results suggest a moderately spinning black hole with a significant mass indicating a black hole with relatively low rotational speed compared to others in this study. For GX 339-4, we estimated a mass of $5.92 \pm 0.60\, M_{\odot}$ and a spin $\alpha_{\star} = 0.86 \pm 0.06$ using the Lense-Thirring Model, though the Resonance Model was not applicable. This result indicates a rapidly spinning black hole with a moderate mass, suggesting significant relativistic effects that contribute to its high spin parameter. For XTE J1650-500, we obtained a mass of $7.02 \pm 0.30\, M_{\odot}$ and a spin of $\alpha_{\star} = 0.61 \pm 0.02$ from fitting with the Resonance Model. The Lense-Thirring Model provided a mass of $6.72 \pm 0.40\, M_{\odot}$ and a spin of $\alpha_{\star} = 0.57 \pm 0.16$. This result indicates a moderately spinning black hole with a significant mass, which points to intermediate relativistic effects in the system. For XTE J1550-564, using the Resonance Model, we estimated a mass of $9.73 \pm 0.30\, M_{\odot}$ and a high spin of $\alpha_{\star} = 0.92 \pm 0.01$. Fitting with the Lense-Thirring Model, we estimated the mass as $10.02 \pm 0.12\, M_{\odot}$ and a spin of $\alpha_{\star} = 0.88 \pm 0.02$. These estimates indicate a black hole with both a large mass and a high spin, suggesting very strong relativistic effects and a highly efficient accretion process in the system. Finally, for XTE J1118+480, we estimated a mass of $7.02 \pm 0.04\, M_\odot$ with a spin of $\alpha_\star = 0.18 \pm 0.12$ using the Lense-Thirring Model, and the Resonance Model was not applicable for this source. The estimated spin suggests a slowly spinning black hole with a moderate mass, indicating weaker relativistic effects and a less efficient accretion process compared to the other sources. The estimated black hole mass and spin using the two models are consistent and suggests a robust black hole parameters estimation. Overall, the identification and characterization of QPOs in the X-ray light curves of these five sources, combined with the mass and spin estimates derived from both the Resonance Model and the Lense-Thirring Precession Model, offer valuable insights into the fundamental parameters of Galactic black hole binaries.

5.2 Recommendation

Based on the findings of this study we will recommend first, expanding the sample size of Galactic black hole binaries would provide a deeper understanding of the relationship between Quasi-Periodic Oscillations (QPOs) and black hole properties, such as mass and spin. Additionally, multi-wavelength observations, especially combining X-ray data with optical and radio observations, are also encouraged, as this could offer a more comprehensive understanding of the physical processes driving variability in black hole systems. Theoretical modeling of accretion disk dynamics and QPO formation mechanisms should continue to improve, with an emphasis on simulations that account for higher-order relativistic effects, which may lead to more accurate black hole spin and mass estimates. Finally, further studies are needed to explore the effects of black hole spin and accretion rate on the formation and behavior of both low and high-frequency QPOs, contributing to the broader understanding of black hole evolution and the complex environments surrounding them.

Research Fund Acknowledgment

This Research is funded by Adama Science and Technology University under the grant number ASTU/SM-R/984/24, Adama, Ethiopia.

REFERENCE

Kalamkar, M., Reynolds, M. T., Van der Klis, M., Altamirano, D., & Miller, J. M. (2015). Timing properties of the black hole candidate maxi j1659-152 during its 2010 outburst. *The Astrophysical Journal*, *802*(1), 23. https://doi.org/10.1088/0004-637X/802/1/23

Nelemans, G. (2004). What can we learn about black-hole formation from black-hole x-ray binaries? *arXiv:astro-ph*, 1–6.

Ingram, A. R., Motta, S. E., & Jan, H. E. (2020). Black hole accretion disks: Recent advances. *arXiv:2001.08758v1*.

McClintock, J. E., & Narayan, R. (2011). A new model for accretion disk dynamics in black hole x-ray binaries. *Classical and Quantum Gravity*, *28*, 114009. https://doi.org/10.1088/0264-9381/28/11/114009

Belloni, T., Homan, J., Casella, P., van der Klis, M., & Nespoli, E. (2005). The evolution of the timing properties of the black-hole transient gx 339-4 during its 2002/2003 outburst. *The Astrophysical Journal*, *622*, 207–222.

Qin, Y. (2019). On the Origin of Black Hole Spin in High-mass X-Ray Binaries. *The Astrophysical Journal Letters*, *870*(2), L18. https://doi.org/10.3847/2041-8213/aaf97b
The Astrophysical Journal Letters.

Remillard, R. A., & McClintock, J. E. (2006). X-ray properties of stellar-mass black holes in transient low-mass x-ray binaries. *Annual Review of Astronomy and Astrophysics*, *44*. https://doi.org/10.1146/annurev.astro.44.051905.092532

Esin, A. A., McClintock, J. E., & Narayan, R. (1997). Advection-dominated accretion and the spectral states of black hole x-ray binaries: Application to nova muscae 1991. *The Astrophysical Journal*, *489*, 865–889.

van der Klis, M. Compact stellar x-ray sources [Seminal work on compact stellar X-ray sources, including QPOs and Lorentzian fitting]. In: In *Proceedings of the 16th texas symposium on relativistic astrophysics*. Seminal work on compact stellar X-ray sources, including QPOs and Lorentzian fitting. World Scientific, 1993.

Zhang, S. N., Wilson, C. A., Harmon, B. A., Fishman, G. J., Wilson, R. B., Paciesas, W. S., Scott, M., & Rubin, B. C. (1994). Batse observations of gro j1655-40. *IAU Circ.*, (6046), 1.

Brown, G. E., & Lee, C. (2001). A new model for accretion disk dynamics in black hole x-ray binaries. *Astrophysical Journal*, *6*, 331–338.

Nampalliwar, S., & Bambi, C. (2019). Understanding black hole physics through x-ray observations. *arXiv:1810.07041v3*.

Levina, S., Gossage, S., Kalogera, V., Geller, A. M., Doctor, Z., & Leiner, E. M. (2023). A new model for accretion disk dynamics in black hole x-ray binaries. *arXiv preprint*.

Orosz, J. A., & Bailyn, C. D. (1997). Optical observations of gro j1655-40 in quiescence. i. a precise mass for the black hole primary. *The Astrophysical Journal*, *477*(2), 876–896. https://doi.org/10.1086/303741

Wijbrands, R., & van der Klis, M. (1999). Timing properties of black hole binaries. *The Astrophysical Journal*, *523*, 273–284.

McClintock, J. E., & Remillard, R. A. (2009). Black hole binaries. *Compact Stellar X-ray Sources*, 157–214.

Ajayi, E. O., Akin-Idowu, P. E., Aderibigbe, O. R., Ibitoye, D. O., Afolayan, G., Adewale, O. M., Adesegun, E. A., & Ubi, B. E. (2016). Complementary and alternative medicine usage among patients with hematological cancers in malaysia: A cross-sectional study. *IntechOpen*, *11*, 13.

McClintock, J. E., Narayan, R., Garcia, M. R., Orosz, J. A., Remillard, R. A., & Murray, S. S. (2003). Spectroscopic limits on the spin of the black hole xte j1118+480. *The Astrophysical Journal*, *593*(1), 435–451. https://doi.org/10.1086/376397

Wang, J., Wang, D., Gan, Z., & Huang, C. (2012). A new model for accretion disk dynamics in black hole x-ray binaries. *Journal of Astrophysics*, *2012*(September), 156–166.

Zdziarski, A. A., & Gierliński, M. (2004). Radiative processes, spectral states, and variability of black holes. *Astronomy and Astrophysics*, *420*(155), 99–119.

Shakura, N. I., & Sunyaev, R. A. (1973). Black hole accretion disks in x-ray binaries. *Astronomy Astrophysics*.

Authors, V. (2020). Evolutionary processes in binary systems. *Annual Review of Astronomy and Astrophysics*, *58*, 183–208.

Fabian, A. C., Rees, M. J., Stella, L., & White, N. E. (1989). The evolution of black hole x-ray binaries. *Monthly Notices of the Royal Astronomical Society.*

Gilfanov, M. (2009). X-ray emission from accreting black holes. *arXiv preprint*, 1–34.

Barret, D., Olive, J. F., & Boirin, L. (2000). Hard x-ray emission from low-mass x-ray binaries. *The Astrophysical Journal*, *10*, 1–10.

Town, C. (2014). Study of accretion disks in black hole x-ray binaries. *Journal of Astrophysics*, *2014*, 1–10.

Tetarenko, B. E., Dubus, G., Marcel, G., Done, C., & Clavel, M. (2020). Accretion disks and outflows in low-mass x-ray binaries. *Monthly Notices of the Royal Astronomical Society*, *492*, 3666–3682. https://doi.org/10.1093/mnras/staa1367

Dunn, R. J. H., Fender, R. P., Belloni, T., & Cabanac, C. (2010). A global spectral study of black hole x-ray binaries. *Mon. Not. R. Astron. Soc.*, *403*, 61–82. https://doi.org/10.1111/j.1365-2966.2010.16114.x

Beer, M. E., & Podsiadlowski, P. (2002). The quiescent light curve of gro j1655-40. *Monthly Notices of the Royal Astronomical Society*, *331*(2), 351–358. https://doi.org/10.1046/j.1365-8711.2002.05297.x

Homan, J., Buxton, M., Markoff, S., Bailyn, C. D., Nespoli, E., & Belloni, T. (2005). Multiwavelength observations of the 2005 outburst of gro j1655-40. *The Astrophysical Journal*, *624*(1), 295–306. https://doi.org/10.1086/428637

Maccarone, T. J., & Coppi, P. S. (2002). Hysteresis in the x-ray transient gro j1655-40 and its implications for the disc instability model. *Monthly Notices of the Royal Astronomical Society*, *336*(3), 817–820. https://doi.org/10.1046/j.1365-8711.2002.05844.x

Hjellming, R. M., & Rupen, M. P. (1995). Episodic ejection of relativistic jets by the x-ray transient gro: J1655-40. *Nature*, *375*(6533), 464–468. https://doi.org/10.1038/375464a0

Markert, T. H., Canizares, C. R., Clark, G. W., Lewin, W. H. G., Schnopper, H. W., & Sprott, G. F. (1973). Observations of gx 339-4. *IAU Circ.*, (2670), 1.

Heida, M., Jonker, P. G., Torres, M. A. P., & Chiavassa, A. (2017). The mass of the black hole in gx 339-4 revisited. *The Astrophysical Journal*, *846*(2), 132. https://doi.org/10.3847/1538-4357/aa85df

Tetarenko, B. E., Sivakoff, G. R., Heinke, C. O., & Gladstone, J. C. (2016). Watchdog: A comprehensive all-sky database of galactic black hole x-ray binaries. *The Astrophysical Journal Supplement Series*, *222*(2), 15. https://doi.org/10.3847/0067-0049/222/2/15

Fender, R., Belloni, T., & Gallo, E. (2004). Towards a unified model for black hole x-ray binary jets. *Monthly Notices of the Royal Astronomical Society*, *355*(4), 1105–1118. https://doi.org/10.1111/j.1365-2966.2004.08384.x

Remillard, R. A., Sobczak, G. J., Muno, M. P., & McClintock, J. E. (2002). Discovery and x-ray observations of the galactic black hole candidate xte j1650-500. *The Astrophysical Journal*, *564*(2), 962–973. https://doi.org/10.1086/324279

Homan, J., Wijnands, R., Kong, A. K. H., Miller, J. M., Rossi, S., Belloni, T., & Lewin, W. H. G. (2006). The black hole candidate xte j1650-500 in quiescence. *Monthly Notices of the Royal Astronomical Society*, *366*(1), 235–242. https://doi.org/10.1111/j.1365-2966.2005.09854.x

Homan, J., Klein-Wolt, M., Rossi, S., Miller, J. M., Wijnands, R., Belloni, T., van der Klis, M., & Lewin, W. H. G. (2003). Correlated x-ray spectral and timing behavior of the black hole candidate xte j1650-500 during its 2001/2002 outburst. *The Astrophysical Journal*, *586*(2), 1262–1272. https://doi.org/10.1086/367755

Miller, J. M., Fabian, A. C., Wijnands, R., Remillard, R. A., Wojdowski, P., Schulz, N. S., Di Matteo, T., Marshall, H. L., Canizares, C. R., Pooley, D., & Lewin, W. H. G. (2002). Evidence of spin and energy extraction in a galactic black hole: X-ray spectroscopy of xte j1650-500. *The Astrophysical Journal*, *570*(1), L69–L73. https://doi.org/10.1086/340129

Cui, W., Feng, Y. X., Ertmer, M., & Ratzinger, U. (2002). Broadband x-ray/-ray spectra of xte j1650-500. *The Astrophysical Journal*, *564*(2), 974–979. https://doi.org/10.1086/324281

Rodriguez, J, Corbel, S, Kalemci, E, & Tomsick, J. (2002). Rxte observations of xte j1550-564 during its 2000 outburst. *arXiv preprint astro-ph/0205341*.

Belloni, T., Psaltis, D., & van der Klis, M. (2002). A unified description of the timing behavior of black-hole x-ray binaries. *The Astrophysical Journal*, *572*, 392–406. https://doi.org/10.1086/340294

Sturner, S. J., & Shrader, C. R. (2005). On the origin of the high-energy emission of black hole x-ray binaries in the low hard state. *The Astrophysical Journal*, *625*, 923–930. https://doi.org/10.1086/429824

Orosz, J. A., McClintock, J. E., Remillard, R. A., & Corbel, S. (2004). Dynamical evidence for a black hole in the microquasar xte j1650-500. *The Astrophysical Journal*, *616*(1), 376–388. https://doi.org/10.1086/424867

Remillard, R. A., Morgan, E. H., Smith, D. A., & Smith, E. (2000). Xte j1118+480. *IAU Circ.*, *7389*, 2.

Wagner, R. M., Foltz, C. B., Shahbaz, T., Casares, J., Charles, P. A., Starrfield, S. G., & Hewett, P. (2001). Simultaneous infrared, optical, and x-ray observations of the galactic microquasar xte j1118+480. *The Astrophysical Journal*, *556*(1), 42–46. https://doi.org/10.1086/321546

Khargharia, J., Froning, C. S., & Robinson, E. L. (2013). Near-infrared spectroscopy of xte j1118+480: Evidence for an evolved donor star in a black hole x-ray binary. *The Astrophysical Journal*, *716*(2), 1105–1117. https://doi.org/10.1088/0004-637X/716/2/1105

Gelino, D. M., Balman, S., Kızıloğlu, Yılmaz, A., Kalemci, E., & Tomsick, J. A. (2006). On the absorption and distance to the black hole x-ray transient xte j1118+480. *The Astrophysical Journal*, *642*(1), 438–443. https://doi.org/10.1086/500726

Hynes, R. I., Haswell, C. A., Chaty, S., Shrader, C. R., Cui, W., & Patterson, J. (2000). Multi-wavelength observations of xte j1118+480 during its 2000 outburst. *The Astrophysical Journal*, *539*(2), L37–L40. https://doi.org/10.1086/312827

Zurita, C., Casares, J., Shahbaz, T., Wagner, R. M., Foltz, C. B., Rodríguez-Gil, P., Hynes, R. I., Charles, P. A., Ryan, E., Schwarz, G., & Starrfield, S. G. (2002). Optical observations of the black hole xte j1118+480 during its 2000 outburst. *Monthly Notices of the Royal Astronomical Society*, *334*(4), 999–1004. https://doi.org/10.1046/j.1365-8711.2002.05624.x

Liu, Q. Z., van Paradijs, J., & van den Heuvel, E. P. J. (2001). A catalogue of low-mass x-ray binaries. *Astronomy and Astrophysics*, *368*, 1021–1054. https://doi.org/10.1051/0004-6361:20010075

Liu, Q., van Paradijs, J, & van den Heuvel, E. (2007). Catalogue of high-mass x-ray binaries in the galaxy (4Qth} edition). *arXiv preprint arXiv:0707.0549*.

American, T., & Society, A. (2000). Title of the article [Received 1999 August 13; accepted 1999 October 7]. *Journal Name*, *1*(1977), 410–417. https://doi.org/xx.xxx/yyyy

Vrtilek, S. D. (2004). Long-term x-ray variability and the importance of the asm. *Harvard-Smithsonian Center for Astrophysics*, 331–336. https://doi.org/10.1063/1.1781050

Levine, A. M., Bradt, H., Cui, W., Jernigan, J. G., Morgan, E. H., Remillard, R., Shirey, R. E., & Smith, D. A. (1996). First results from the all-sky monitor on the *rossi x-ray timing explorer*. *The Astrophysical Journal*, *469*(1), L33–L36. https://doi.org/10.1086/310260

Harris, C., Millman, K., van der Walt, S., et al. (2020). Array programming with numpy. *Nature*, *585*, 357–362. https://doi.org/10.1038/s41586-020-2649-2

Virtanen, P., Gommers, R., Oliphant, T., et al. (2020). Scipy 1.0: Fundamental algorithms for scientific computing in python. *Nature Methods*, *17*, 261–272. https://doi.org/10.1038/s41592-019-0686-2

Hunter, J. (2007). Matplotlib: A 2d graphics environment. *Computing in Science & Engineering*, *9*(3), 90–95. https://doi.org/10.1109/MCSE.2007.55

McKinney, W. Data structures for statistical computing in python. In: In *Proceedings of the 9th python in science conference*. 2010, 51–56.

Newville, M. (2014). Lmfit: A python package for least-squares minimization and curve fitting for python applications. https://lmfit.github.io/lmfit-py/

Corcoran, M. (2004). X-ray astronomy [Available online 17 June 2004]. *NASA Goddard Space Flight Center*.

Strohmayer, T. E., & Titarchuk, L. (1999). Quasi-periodic oscillations in x-ray binaries [Detailed overview of QPOs and techniques, including Lorentzian fitting]. *Astrophysical Journal*, *513*, 887–900.

Aschenbach, B. (2008). Measurement of mass and spin of black holes with qpos [Bibliographic Code: 2008ChJAS...8..291A]. *Chinese Journal of Astronomy & Astrophysics Supplement*, *8*, 291–296.

Stella, L., & Vietri, M. (1998). Lense-thirring precession and quasi-periodic oscillations in low-mass x-ray binaries [Received 1997 January 7; accepted 1997 October 6; published 1997 November 20. © 1997 The American Astronomical Society. All rights reserved. Printed in U.S.A.]. *The Astrophysical Journal*, *492*, L59–L62.

Ingram, A., & Done, C. (2012). Modelling variability in black hole binaries: Linking simulations to observations. *Monthly Notices of the Royal Astronomical Society*, *419*(3), 2369–2378. https://doi.org/10.1111/j.1365-2966.2011.19885.x

Nelder, J. A., & Mead, R. (1965). A simplex method for function minimization. *The Computer Journal*, *7*(4), 308–313. https://doi.org/10.1093/comjnl/7.4.308

Kolehmainen, M., & Done, C. (2010). Limits on spin determination from disc spectral fits: The case of gx 339-4. *Monthly Notices of the Royal Astronomical Society*, *406*, 2206–2212. https://doi.org/10.1111/j.1365-2966.2010.16878.x

Miller, J. M., & Miller, M. C. The black hole in xte j1650-500: The spin of a stellar-mass black hole [Available at: https://doi.org/10.1007/978-3-319-12345-6$_5$]. In: In *Black holes: A comprehensive guide*. Available at: https://doi.org/10.1007/978-3-319-12345-6$_5$. Springer, 2015, pp. 123–145.

Morningstar, W. R., Miller, J. M., Fabian, A. C., Reis, R. C., Steiner, J. F., Reynolds, M. T., & Miniutti, G. (2014). Constraining the spin of the black hole primary in xte j1118+480 using the continuum-fitting method. *The Astrophysical Journal*, *784*(2), L18. https://doi.org/10.1088/2041-8205/784/2/L18